MAGIC-TDAS 03-01
000301/AMoralejo

A first estimate of the MAGIC capabilities using the new MC simulation chain

C.Bigongiari, A.Moralejo, V.Scalzotto
<bigongiari@pd.infn.it>,<moralejo@pd.infn.it>,<scalz8@pd.infn.it>

April 10, 2003

Abstract

New versions of the MAGIC simulation programs have been released three months ago, after some bugs were found in both MMCS and the Reflector codes. Since January, the MAGIC Monte Carlo library is being rebuilt from scratch. In this draft we present a first look at the outcome of the new simulation chain. The first results seem to indicate that the sensitivity of the instrument is not as high as claimed by previous studies. Nevertheless, this work is rather preliminar and incomplete, and is being distributed with the aim of getting as much feedback as possible from the rest of the collaboration. This is quite urgent, given that a few of the MAGIC contributions to the ICRC (which should be ready in about one month) will be based on the MC results.

Contents

1 Introduction

Once the last release of MAGIC Monte Carlo programs has become available **(Reflector 0.6, Camera 0.6, Corsika MMCS 6.019)**, a re-evaluation of the Telescope capabilities is necessary. The new MC production at Padua has now reached about $32 \cdot 10^6$ showers, most of which have been analysed in some detail for the studies presented in this draft. For the following work, we used a starting sample of **5.2 million of gammas**, **15.6 million protons**, and 7.8 million Helium nuclei (only about 82% of the latter were used, in order to reproduce the known Cosmic Ray composition).

The main parameters of the shower production are the following:

- Zenith angle θ between 0 and about 29°, with flat distribution in $d\cos\theta$. The hadrons were produced in 5° semiaperture cones, centered at values of $\cos\theta = 1.00, 0.99, 0.98,...$ ($\Delta(\cos\theta) = 0.01$), while for the gammas θ was varied in a continuous way.
- Azimuth angle distribution: two discrete values. $\phi = 0°$ (shower coming from South) and $\phi = 90°$ (shower coming from East). The same number of events was generated at each ϕ.
- Shower core distribution: within a circle of 400 m radius for hadrons, and 300 m radius for gammas (the circle is orthogonal to the telescope axis).
- Energy range: from 30 GeV - 30 TeV for hadrons, 10 GeV - 30 TeV for gammas. The spectral index is 2.6 for gammas, 2.75 for protons and 2.62 for Helium.

Each Corsika shower has been used only once. The reflector simulation was run with the telescope pointing towards the direction of the source for the case of gammas, and pointing along the axis of the generation cone (see above) for hadrons.

2 Camera simulation

After reflection of the showers, the camera program has been run over the sample using the up to now standard L1 trigger condition for the MAGIC MC: 4 close-compact next neigbour pixels each above a L0 threshold of 4 mV. The single photoelectron response of the PMs is a gaussian of width 2 ns and height following the probability distribution shown in fig. 1 (as in previous versions of the camera program), which peaks at 1 mV. The pixel discriminator output signal (gate length) is set to a duration of 6 ns. We note that the real value of the latter quantity in the L1 hardware seems to be around 3 ns (according to M. Mariotti). The results shown here will not change much by updating this value, since the only effect will be a slight reduction in the rate of accidental NSB triggers which is anyhow negligible in the data used for this report. We checked that practically no triggered showers are lost by such a change. Any further optimization of the L1 trigger will be difficult with the present MC library. The reason is, that in order to simulate realistically looser trigger conditions we would have to simulate gamma events below 10 GeV and proton events below 30 GeV. Otherwise we would be losing a significant number of events which would trigger if present in the sample (see figs. 3 and 4).

Given the fixing of bugs in the reflector program, the chosen "traditional" L1 trigger setup corresponds now to a much higher trigger efficiency than before: about 7% for gammas, 0.15% for protons and 0.6% for Helium (given the sample described above). Table 1 shows the statistics of triggered events in our MC sample.

Finally, the FADC response is a gaussian of FWHM equal to 5 ns and height 4 ADC counts.

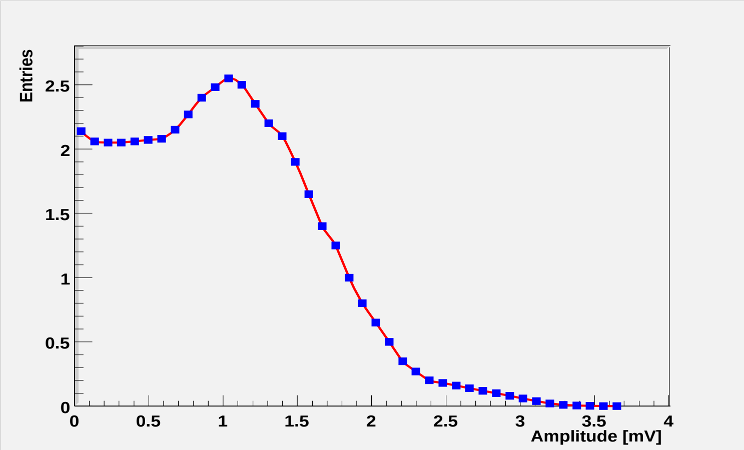

Figure 1: The distribution of the amplitude of the standard PM response function used in the MC camera simulation.

2.1 Night Sky Background and electronic noise

We have used a mean diffuse NSB of 0.09 phe$^-$ per ns per small pixel[1]. No star fields were used in this simulation. The contribution of NSB to the signal in a single FADC slice can be seen in figure 2 for an inner and an outer pixel (all the other pixels follow the same behavior). In the same plot, a funny saturation effect can be observed, which occurs at different amplitudes for inner and outer pixels. We checked that this saturation affects only the NSB and not the signal from shower photons. The origin of this phenomenon seems to be in the NSB database generated by the program *starrespo*, which simulates a limited time of FADC response to the NSB (which is later re-used many times when running the camera). The saturation point would correspond to the maximum NSB fluctuation in this database. In any case, the saturation takes place at a sufficiently low rate (as can be seen from the numbers in the plot) as to be considered unimportant for the results of the present study.

The fluctuations of the pedestal due to electronic noise were set to zero, since we found that most of the camera execution time ($\simeq 90\%$) was lost in calculating the gaussian random numbers (15×577 for each event) needed for this. We will have to introduce a faster way to simulate the electronic noise. Therefore, for the moment we have to keep in mind that the results in this work are probably optimistic since the noise in the pixel signal (both from NSB and from electronics) is underestimated.

2.2 Trigger rate

The resulting trigger rate with the above conditions is about 390 Hz of protons and 70 Hz of Helium nuclei. The contribution of Helium is about half of what we had estimated using the old MC (although we do not know whether the difference is due to the fixed bugs or to some other error in the old estimate). In figure 3 we can see that, although it seems that the chosen impact parameter range is enough to contain the vast majority of triggered protons, we are losing some low energy events (E

[1] This is an outdated value, since it was calculated for a somewhat smaller mirror and lower quantum efficiency than the ones in the present MC (in which the mirror dish was updated to its final design and the QE raised to account for the effect of the coating). The real value of NSB should now be around 0.12 in the same units. We are already running the camera with this value in order to obtain more realistic results soon.

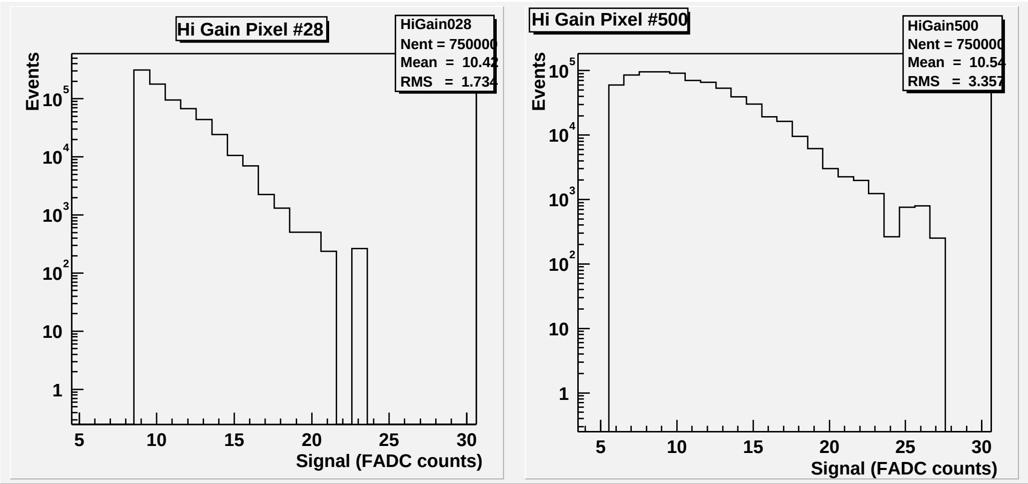

Figure 2: Distribution of the NSB contribution to the signal in one FADC slice of an inner pixel (left) and an outer pixel (right). Mind that in our analysis 3 FADC slices have been integrated (see section 3).

< 30 GeV), and for this reason the rate quoted above is probably underestimated by 5 to 10%. This is not the case for Helium nuclei (because their trigger efficiency at a given energy is lower than for protons). The same effect (see fig. 4, left) occurs in the gamma sample. A number of events below 10 GeV which would trigger are missing in our sample (amounting again to a few percent of all triggers). Bear in mind that the histogram in fig. 4, peaking at 30 GeV, represents $\log_{10} E$ and therefore it is not a differential energy spectrum (because bins have different widths ΔE). If we make the true differential spectrum of triggered gammas in our sample, we get a peak energy of 18 GeV. Finally, it seems that the maximum off axis angle in which the hadronic showers are generated (5 degrees) is also large enough as to contain nearly all the possible cosmic ray triggers (see figure 5).

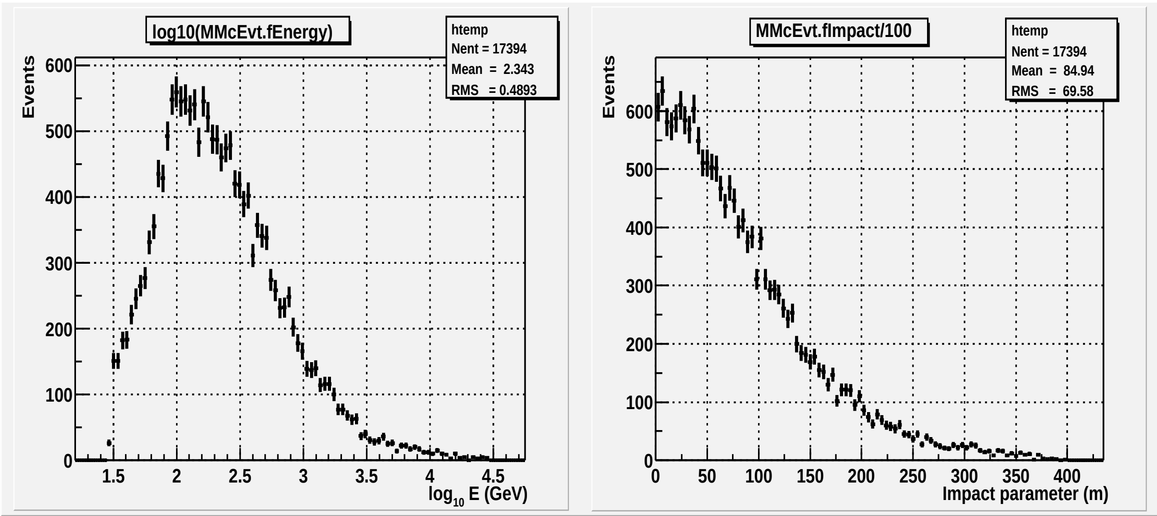

Figure 3: Energy and impact parameter distribution of triggered protons.

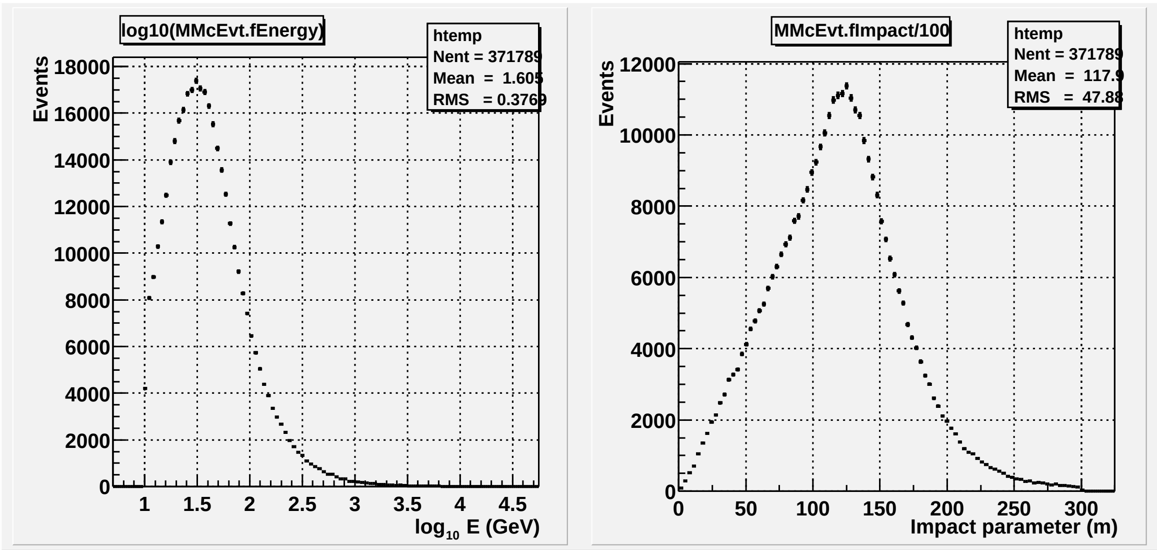

Figure 4: Energy and impact parameter distribution of triggered gammas.

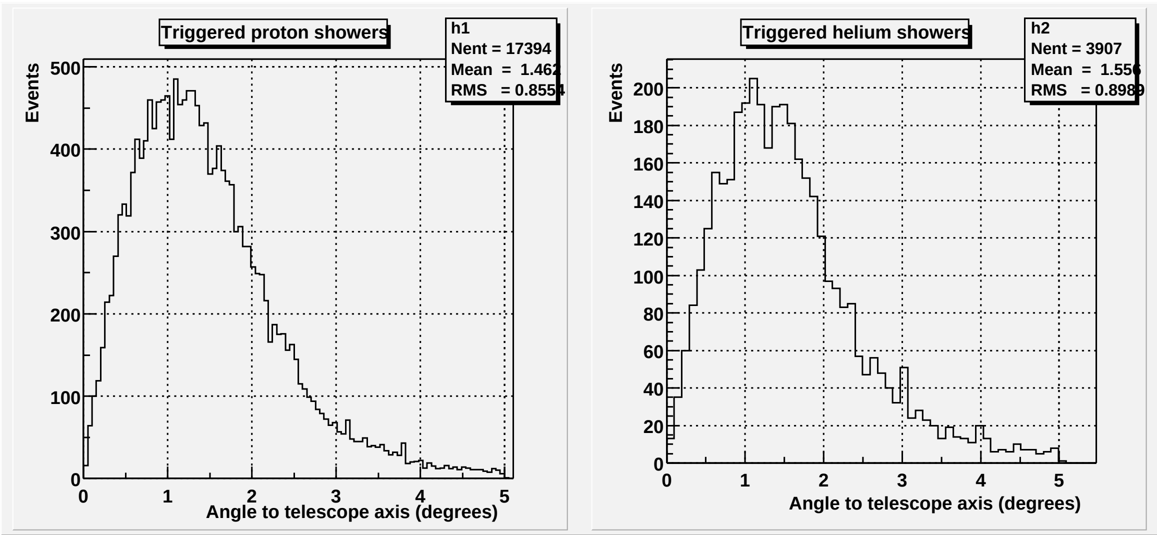

Figure 5: Distributions of the angle between the telescope axis and the axis of triggered hadronic showers.

Bin	θ interval (°)	ϕ (°)	Gammas	Protons	Helium
0	0 - 5.73	0	14831	724	164
		90	14217	710	155
1	5.73 - 9.94	0	15098	726	158
		90	14175	732	152
2	9.94 - 12.84	0	15392	721	145
		90	14118	712	170
3	12.84 - 15.20	0	15464	733	146
		90	13854	686	176
4	15.20 - 17.25	0	15593	673	158
		90	13511	654	164
5	17.25 - 19.09	0	15644	601	104
		90	13363	701	175
6	19.09 - 20.77	0	15591	641	183
		90	13233	666	153
7	20.77 - 22.33	0	15740	665	164
		90	12969	689	150
8	22.33 - 23.79	0	15624	687	140
		90	12726	669	134
9	23.79 - 25.18	0	15690	713	167
		90	12427	654	129
10	25.18 - 26.49	0	15755	647	129
		90	12202	621	134
11	26.49 - 27.75	0	15654	590	157
		90	11743	587	135
12	27.75 - 28.96	0	15484	580	128
		90	11691	612	137
Total	0 - 28.96	0	201560	8701	1943
		90	170229	8693	1964

Table 1: Description of the Monte Carlo sample used in the present analysis. The three columns on the right show the number of triggered events.

3 Data analysis

The signal from each pixel is evaluated by summing the signals from 3 FADC time-slices (second to fourth) in which most of the signal is concentrated. The figure 6 shows the integrated signal of the 15 FADC slices of pixel 90 for several thousands gamma and proton showers. The pedestal value, set in the simulation equal to 10.5 ADC counts, is not subtracted yet in the plot. In the case of protons, the signal is slightly wider, although the difference is difficult to notice unless we add up a large number of events as we have done for the plot. By integrating only 3 out of 15 slices (about 10 ns) we keep most of the signal while adding less background light to the signal. Integrating 3 slices means that the fluctuations due to NSB in the pixel signal will be a factor $\sqrt{3}$ larger than the values histogrammed in fig. 2 for a single slice.

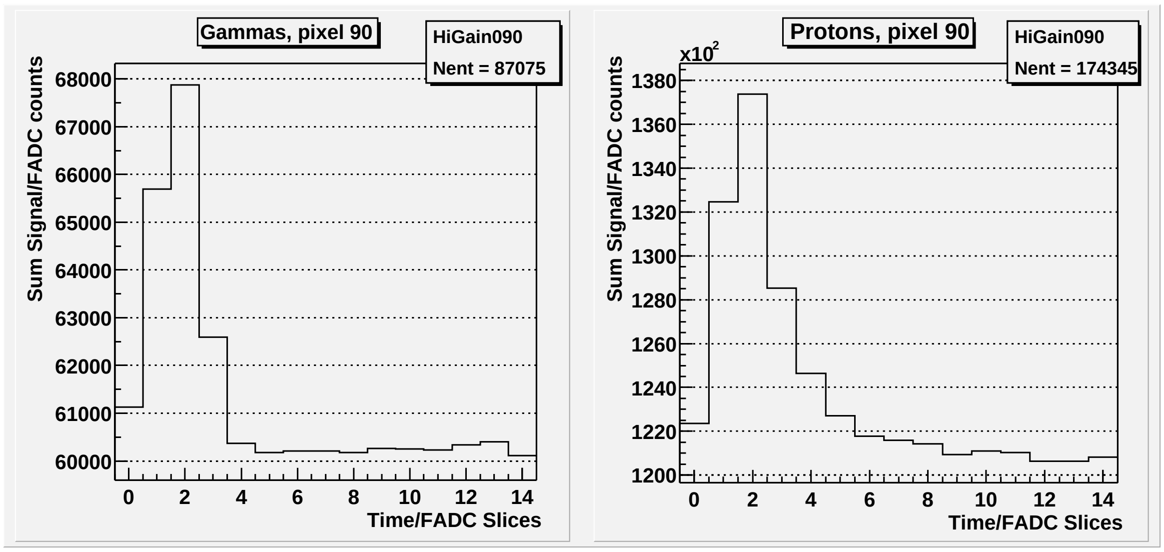

Figure 6: Signal in the FADC of pixel 90 for gamma and proton showers. The curves are the sum of the signals from 5805 gammas and 11623 protons. Pedestal (10.5 counts per event and slice) is not subtracted, and amounts to 60952.5 counts (left) and 122041.5 counts (right).

3.1 Image cleaning

We have applied the standard Image cleaning in Mars. In a first step, we select all pixels which are above pedestal by at least 3 σ (the RMS of the fluctuations of the noise). Of those, only the ones having at least one neighbour fulfilling the same condition are kept. These are called "core pixels". Finally, pixels above 2.5 σ and with a neighboring core pixel are also included in the set of pixels to be used in the analysis. The quoted tail cuts are valid for the inner pixels. For the outer ones, the cut values are raised proportionally to the pixel area (about twice that of inner pixels). This "democratic" image cleaning suggested by Wolfgang Wittek has been implemented in order not to bias the image, since in this way the cut in every pixel corresponds to the same "signal density" (it has the consequence that the noise supression is stronger in outer pixel, but this should not be a problem).

3.2 Image analysis

A "standard" (Hillas-like) Image analysis has been performed, including the third moments of the phe^- distribution on the camera. For the gamma / hadron separation we have used the following set of variables:

- $Width$
- $Length$
- $Size$: sum of signal in all pixels after cleaning (ADC counts).
- $Dist$: Distance from the image center of gravity to the camera center (where the gammas come from).
- $Conc$: ratio (sum of signal in two highest pixels) / Size
- $Alpha$: measured in the range between -90 and 90°. Therefore it contains no head-tail information (would have the same value if, for a given shower, head and tail were flipped). The head-tail information is contained in the next variable.
- $M3Long\cdot$ sign($CosDeltaAlpha$) : Third moment along major axis. It is a measure of the longitudinal asymmetry of the shower, with a sign which is positive is the shower "head" is closer to the source direction than the shower "tail", and negative otherwise.
- floor(0.5+cos($TelescopeTheta$)/0.01) : cosine of the zenith angle of telescope pointing, rounded to 1/100, so that we get the same distribution for gammas (which have a continuous distribution of TelescopeTheta) and protons (which do not).

For details on the precise definition of these variables, check TDAS 02-03 (in the notation used there, what in *Mars 0.8* is called $CosDeltaAlpha$ corresponds to $(\vec{a}\cdot\vec{d})/|\vec{a}\cdot\vec{d}|$, and $M3Long$ is called ASYM). Only the variables shown in the list (and not their errors) have been used here. In order to decide which of the available variables to use, we have simply started from a set of five *(Alpha, Dist, Length, Width and Size)* and then we tried to add other variables, accepting them if the result became better (in terms of Q, see below) and rejecting them otherwise. Among the rejected variables were $Conc1$ (ratio of signal in highest pixel to $Size$), $M3Trans$ (third moment along the image minor axis) and the azimuthal angle ϕ at which the telescope points. The case of the last variable is strange, since although we did not expect it to contribute much to separation, it actually produced a significant worsening in the performance of the method (which we do not understand).

In our MC sample, the image parameters were succesfully reconstructed for 99.99% of the gammas, 97.7% of protons, and 95.9% of the helium nuclei.

3.3 Optimization of gamma / hadron separation cuts

The optimization of the gamma / hadron separation has been done using Thomas Hengstebeck's implementation of the Random Forest method, which he recently included in Mars. The eight variables listed above were fed into the routine, setting the number of trees to 100. Other parameters of the algorithm were left unchanged at their default values in the Mars macro RanForest.C (playing around a little bit with them did not produce any significant improvement in the results).

The proton, helium and gamma samples have been divided each in two, a training sample and a test sample, taking care that the events in both had (within random fluctuations) the same composition in all parameters (θ, ϕ, energy...). For the case of hadrons, two thirds of all available data were assigned to the training sample and the rest to the test sample. About 18 % of the Helium triggers were excluded from both the training and test samples so that their composition is comparable to that of real CR. In the case of gammas, we decided in the end not to use all the available events (see table 1) because the Random Forest became too slow and anyway the quality of the achieved separation did not improve, given that it is limited by the smaller sample (which is that of the hadrons). For instance, for the sample with no size cut only one each of every 20 gamma showers was used. This ratio was changed in the samples with Size cuts so that we always had at least 10^4 gammas for the training and the same for the test.

The Random Forest method tags ech event with a "*Hadronness*" value ranging from 0 (gamma-like event) to 1 (hadron-like event). Obviously the gamma / hadron separation cut is of the form $Hadronness < x$. As a measure of the efficiency of a given cut we will take the usual definition of "quality factor" :

$$Q = \frac{\varepsilon_\gamma}{\sqrt{\varepsilon_h}} \tag{1}$$

where the efficiencies ε_γ, ε_h are equal to the ratio of the number of events after the cut to the number before the cut (and hence refer exclusively to the effect of the γ/h separation procedure). In general we will apply in our analysis the cut which maximizes Q.

4 Evaluation of Sensitivity

In order to estimate the sensitivity of MAGIC for detection of point-like gamma ray sources, we search for the minimum integral flux $\phi^{min}_{E>E_0}$ (assuming a diferential power law spectrum with index $\alpha = 2.6$) which, in 50 hours of observation, results in a number of detected photons equal to 5 times the standard deviation of the CR background fluctuations. By "detected" photons and CR background we mean those showers surviving the gamma / hadron separation cuts (where hadrons include only protons and Helium nuclei):

$$R^{min}_\gamma \cdot t_{50} = 5 \cdot \sqrt{R_h \cdot t_{50}} \tag{2}$$

, being R^{min}_γ the rate of gamma rays and R_h the rate of hadrons after the whole analysis chain, and $t_{50} = 50$ hours. From (2), R^{min}_γ can be calculated and the minimum detectable flux $\phi^{min}_{E>E_0}$ determined. The value of E_0 can be chosen arbitrarily (since we assume a single power-law with fixed spectral index), but it would not make much sense to choose it outside the energy region where the telescope is sensitive. For the full MC sample, we have taken E_0 to be the peak energy of the differential energy spectrum after trigger[2]. This definition of sensitivity does not mean that in 50 h time we will get as much as a 5 σ detection from a source emitting a flux $\phi^{min}_{E>E_0}$, since a proper calculation of the statistical significance of the signal has to consider both the fluctuations of the ON source "counts" and those of the estimated background, and hence depends also on the method for estimating the latter (either OFF source observations, modelling the Alpha distribution of the background in the ON source data...).

Taking into account that our gamma sample is produced starting at 10 GeV, with impact parameter

[2] If one takes instead the energy spectrum after the γ/h separation, the E_0 value stays nearly the same. For practical reasons we have preferred the former.

distributed in an area $A = \pi \cdot (300\ \mathrm{m})^2$, the rate of gammas is given by:

$$R_\gamma = \phi_{>10\ \mathrm{Gev}} \cdot \frac{N_{\gamma,\ final}}{N_{\gamma,\ produced}} \cdot A \tag{3}$$

, where $N_{\gamma,\ produced}$ and $N_{\gamma,\ final}$ are respectively the total number of generated MC gammas (before trigger) and the number of those surviving the whole analysis chain. The formula above assumes that the MC events are generated from 10 GeV up to an arbitrarily high energy; the fact that the MC library reaches only up to 30 TeV would mean a negligible correction of about 3 parts in a million. From (2) and (3) and using $\phi_{E>E_0} = \phi_{E>10\ \mathrm{GeV}} \cdot (E_0/10\ \mathrm{GeV})^{-1.6}$, we arrive at

$$\phi^{min}_{E>E_0} = \frac{5}{A} \cdot \sqrt{\frac{R_h}{t_{50}}} \cdot \left(\frac{E_0}{10\ \mathrm{GeV}}\right)^{-1.6} \cdot \frac{N_{\gamma,\ produced}}{N_{\gamma,\ final}} \tag{4}$$

To calculate R_h we use the analog of expression (3) for proton and helium, with the following differential spectra:

$$\frac{d\phi}{dE}\ (\mathrm{protons}) = 0.1091 \cdot \left(\frac{E}{1\ \mathrm{TeV}}\right)^{-2.75}\ \mathrm{TeV}^{-1}\ \mathrm{m}^{-2}\ \mathrm{s}^{-1}\ \mathrm{sr}^{-1} \tag{5}$$

$$\frac{d\phi}{dE}\ (\mathrm{helium}) = 0.0660 \cdot \left(\frac{E}{1\ \mathrm{TeV}}\right)^{-2.62}\ \mathrm{TeV}^{-1}\ \mathrm{m}^{-2}\ \mathrm{s}^{-1}\ \mathrm{sr}^{-1} \tag{6}$$

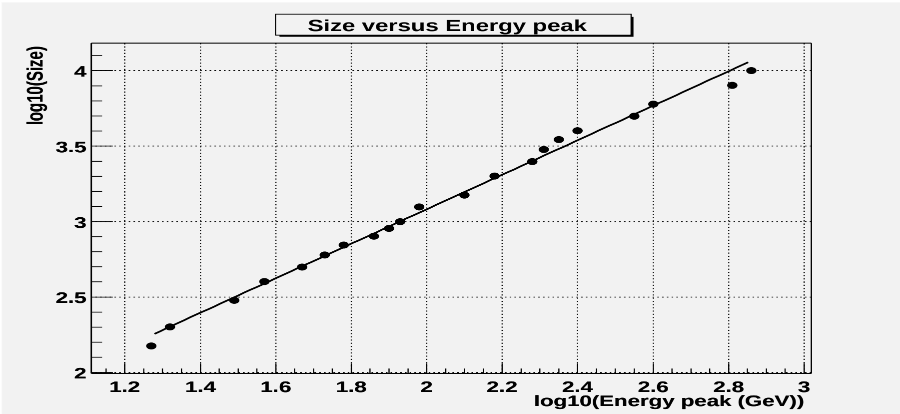

Figure 7: Size cut in function of the energy peak. The linear fit gives: $log_{10}(Size) = (1.144 \pm 0.016) \cdot log_{10}(E_0) + (0.794 \pm 0.033)$, with Size in ADC counts and E_0 in GeV.

We can obtain the MAGIC sensitivity at different energies by artificially increasing the energy threshold via a software cut. For this we have used a cut $Size > S_0$, with $S_0 = 0$ (no cut), 300, 500, 1000 and 2000 ADC counts. We have associated each size cut value to the peak of the differential energy spectrum of the remaining events after the cut, which will be the E_0 used in expression (4) for these samples. The relation between Size-cut and Energy peak is shown in the figure 7, and seems rather linear.

The Size values above are in units of ADC counts. It is rather helpful to know the approximate conversion factor between these and photoelectrons. This can be found comparing the $Size$ values with the number of photoelectrons produced by the light from the shower, which is a number available in the Monte Carlo files (*fPhotElfromShower*). In figure 8 we show the **number of photoelectrons coming from the shower** versus the **image size**. The expected behaviour is linear, since the image cleaning (ideally) must have removed the contribution from NSB photons and left on the camera only the light from the shower. Actually the plot is not linear, due to two effects: for low amplitudes the background fluctuations become comparable to the signal (hence we expect the correlation to become lousy for small Size), while at high amplitudes the saturation of the ADC sets in [3] and the correlation is no longer linear. To calculate an approximate conversion factor between photoelectrons and ADC counts we simply make the histogram of $(Size/\Sigma\ ph.e.)$ for light yields between 400 and 1000 ph.e. (fig. 8, right), from which we obtain 1 $ph.e. = 3.30 \pm 0.28$ ADC counts.

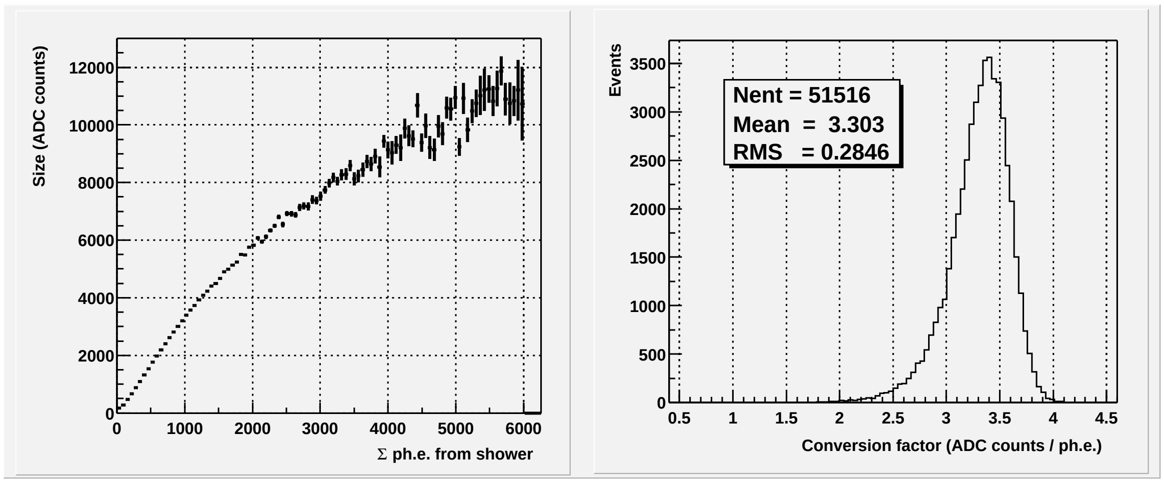

Figure 8: Estimate of the equivalence between photoelectrons and ADC counts in the MC.

Table 2 presents the results of the sensitivity calculation for the different *Size* cuts. Figures 10 to 14 summarize the output of the Random Forest algorithm for the same five samples. The quality factor in the first three samples presents a rather flat maximum around a gamma efficiency of about $\varepsilon_\gamma = 0.5$, which has been chosen as the optimal cut for this analysis. In the last two energy bins, no maximum is clearly visible, due to the scarce statistics, so we have kept somehow arbitrarily the cut at the same gamma efficiency $\varepsilon_\gamma = 0.5$. In the last bin only five proton and no helium showers are left after the cut. Hence this last point is not very reliable. The bin before last keeps enough hadrons after cut (29) as to not not expect any significant change in the result by just adding more statistics. Bear in mind that the hadron efficiencies enter expression 4 (through R_h) under a square root. Some small improvement could nevertheless come from adding statistics to the hadron training samples of the last three bins (composed now by about 8900, 5100 and 2500 events) since according to Thomas Hengstebeck, these might be too small samples for the random forest method to reach its best performance.

Not included in this analysis is the effect of the electron background. Anyhow, we are working on this issue, and a preliminar study indicates that with a modest supression via the *Alpha* parameter, its contribution to the total background will be almost negligible.

[3]We have no low gain in the MC, something which should be fixed in future versions of the camera.

Size cut	0	300	500	1000	2000
Hadronness cut	0.166	0.161	0.0863	0.0374	0.0023
Q	2.1	2.8	3.3	4.7	7.8 ?
ε_{γ}	0.5	0.5	0.5	0.5	0.5
ε_{proton}	$5.86 \cdot 10^{-2}$ (330 / 5634)	$3.29 \cdot 10^{-2}$ (156 / 4744)	$2.4 \cdot 10^{-2}$ (90 / 3769)	$1.3 \cdot 10^{-2}$ (27 / 2130)	$5.0 \cdot 10^{-3}$ (5 / 1003)
ε_{helium}	$6.29 \cdot 10^{-2}$ (63 / 1001)	$2.54 \cdot 10^{-2}$ (21 / 827)	$1.5 \cdot 10^{-2}$ (10 / 674)	$4.8 \cdot 10^{-3}$ (2 / 420)	– (0 / 229)
Proton rate after cuts (Hz)	22.0	10.4	6.0	1.8	0.33
Helium rate after cuts (Hz)	4.24	1.41	0.7	0.13	–
$\frac{N_{\gamma,\ produced}}{N_{\gamma,\ final}}$	28.0	43.5	73.3	170.4	418.9
Peak Energy E_0	15 GeV	31 GeV	50 GeV	83 GeV	151 GeV
$\phi^{min}_{E>E_0}$ ($\mathrm{cm}^{-2}\ \mathrm{s}^{-1}$)	$3.12 \cdot 10^{-10}$	$1.01 \cdot 10^{-10}$	$6.16 \cdot 10^{-11}$	$3.3 \cdot 10^{-11}$	$1.3 \cdot 10^{-11}$
Equivalent number of photons in 50 h	10860	7290	5616	2912	1216

Table 2: Sensitivity of MAGIC for different cuts in *Size*, using the analysis described in the text. The numbers in brackets below the gamma/hadron separation cut efficiencies for protons and helium are the number of events after / before the cut (test sample only). The results for the highest energy bin are very uncertain, since they are based in very few hadron showers surviving the cut.

5 Results and discussion

In figure 9 the sensitivity calculated above as a function of energy is plotted, together with the result shown in the MAGIC proposal and with the claimed sensitivities of other experiments. We can see that the new result is much worse than foreseen in the proposal. Although some bugs were found in the MC (chain) particularly in the reflector, which had a sensible effect on collection areas and trigger rates, the situation has not changed much with regard to the gamma / hadron separation ability of the instrument (if we judge from the quality factors). We are still significantly worse than the proposal in this respect, where quality factors between 7 and 10 were predicted for MAGIC with the PMT camera, using an analysis similar to the one presented here. The differences in sensitivity are further enhanced by the fact that we now know for sure that the estimated background rates in the proposal were far too low due to an error in the angular distribution of the generated hadronic showers. From p. 170 of the proposal, an expected trigger rate of protons of 13 Hz (!) is quoted for a trigger condition corresponding to a gamma threshold about 30 GeV (comparable to our sample with *Size* > 300 ADC counts, which has a proton rate of 330 Hz before γ/h separation). All other things being equal, just this difference in rate would account for a difference of about a factor 5 in sensitivity. We still do not know the details of this error (since no documentation exists on it apart from some discussions via e-mail), but the people who detected it some years ago (J.C. González and D. Petry) already realized that it produced a big underestimate of rates. This fact, together with a worsening of gamma/hadron separation (of about a factor 2 or three depending on the energy) explains the difference in the estimate of sensitivity.

The error in the absolute background flux does not immediately explain a worsening of the gamma / hadron separation, since quality factors are calculated with respect to the number of events in the starting sample. A part of the effect may be due to the known differences in the MC simulation, mainly the fact that in the proposal the simulated PMT camera was fully equipped with $0.1°\varnothing$ pixels. On the other hand, it is possible that the protons missing in the MC MC sample used in the proposal, were mainly gamma-like (hence making the gamma / hadron separation easier). This is just a guess, which may be confirmed in the future by studying proton samples with different angular distributions around the telescope axis. However, the distributions of image parameters for the gammas and protons in our sample are rather compatible with those on the proposal, as we will see in the next section. This would be in disagreement with that hypothesis.

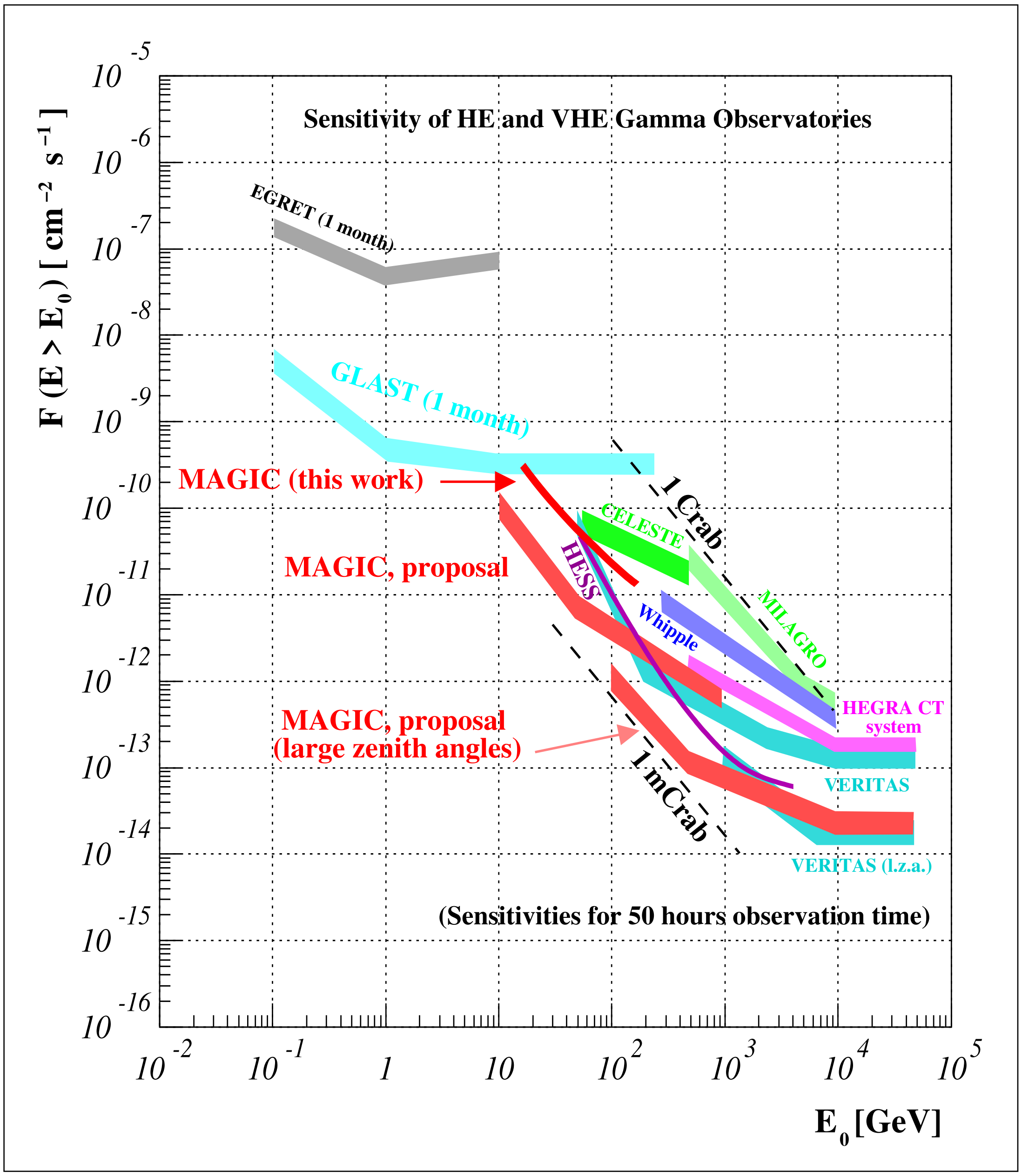

Figure 9: Sensitivity of MAGIC as obtained in this work, compared with other experiments and with the estimate for MAGIC shown in the proposal.

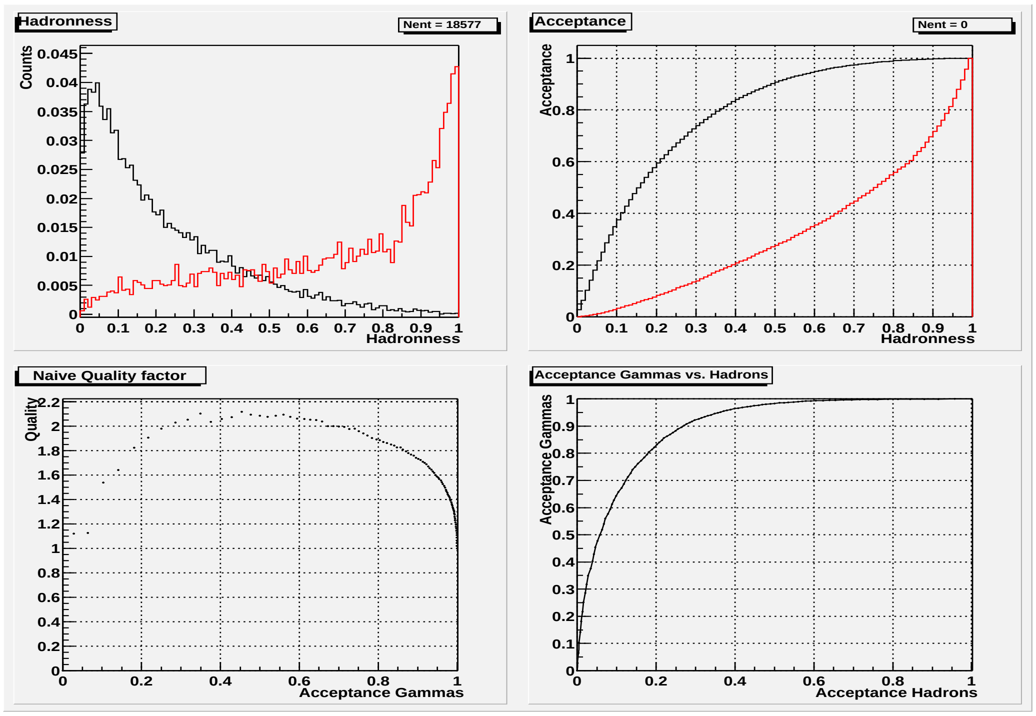

Figure 10: Output of Random Forest for the basic MC sample.

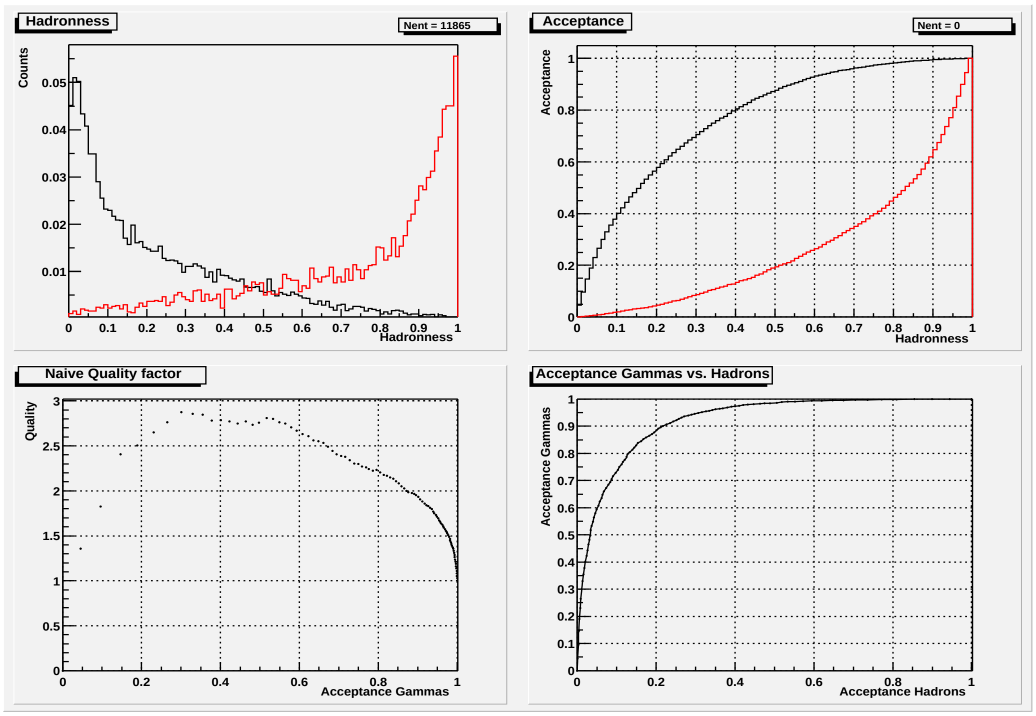

Figure 11: Output of Random Forest for the MC sample with $Size > 300$ ADC counts.

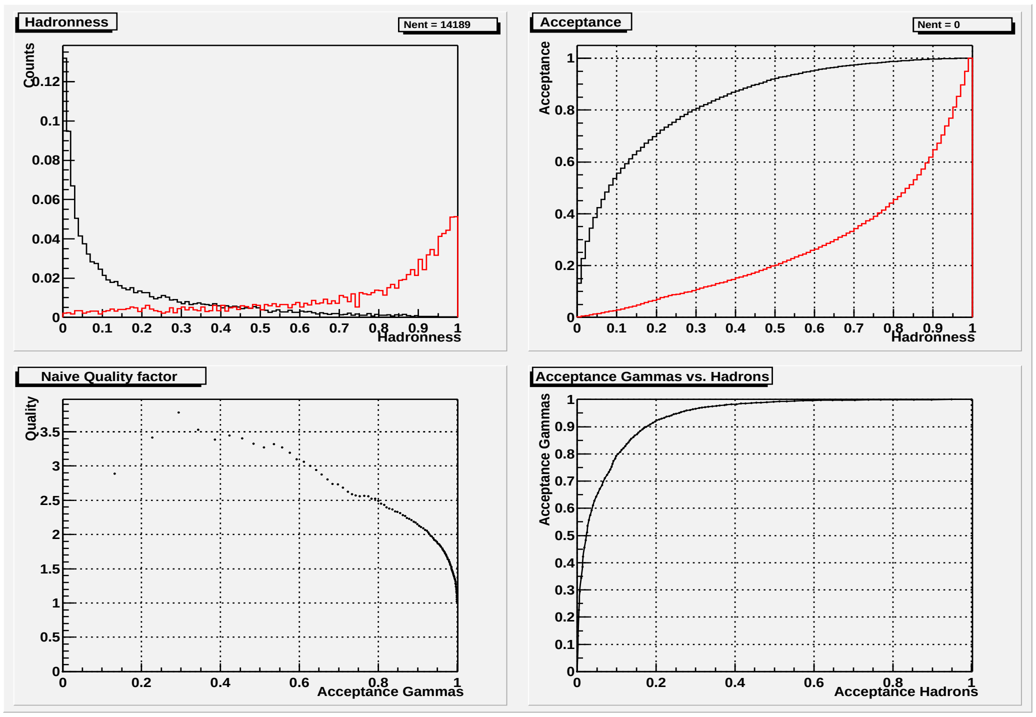

Figure 12: Output of Random Forest for the MC sample with $Size > 500$ ADC counts.

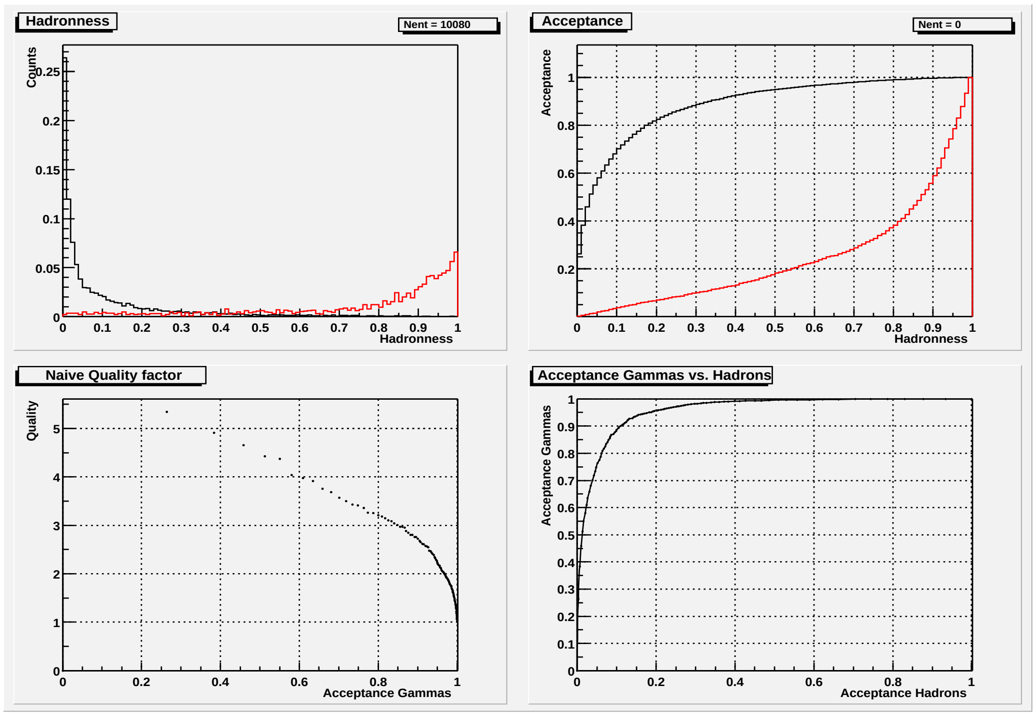

Figure 13: Output of Random Forest for the MC sample with $Size > 1000$ ADC counts.

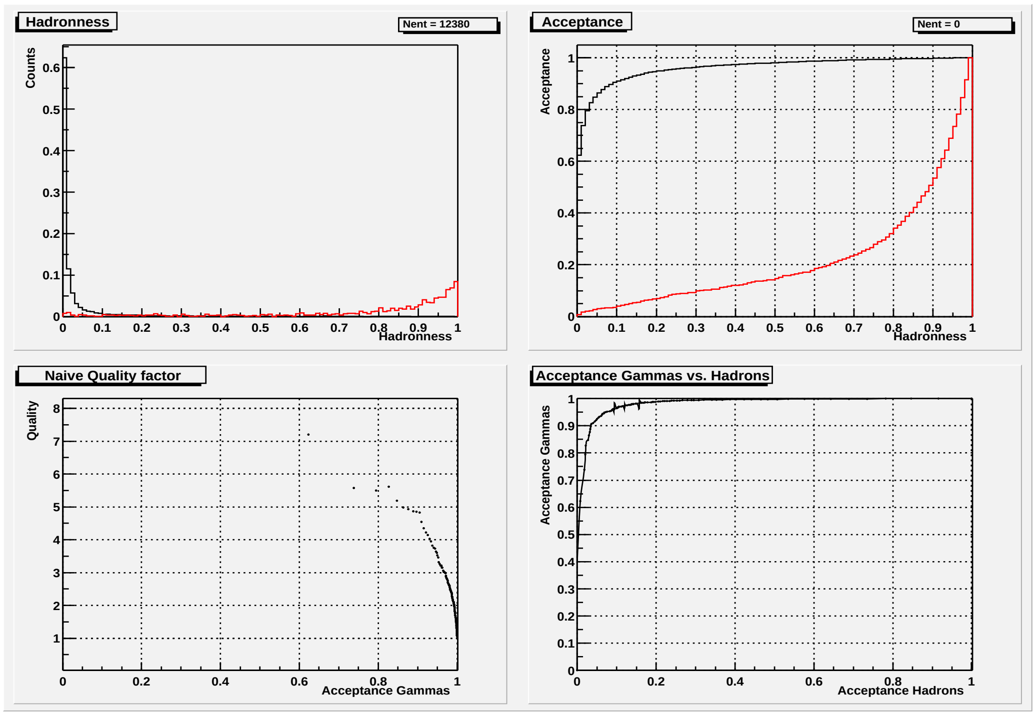

Figure 14: Output of Random Forest for the MC sample with $Size > 2000$ ADC counts.

6 Image Parameters distributions

In this section, we provide some plots showing the behaviour of some of the Image parameters of the new simulated events at different energies. This is of interest for making comparisons with the analogous plots in the proposal (bearing in mind that the plots in the proposal are mostly for the IAPD camera). In our case the energies are not fixed at the values quoted on the plots, but correspond actually to the following ranges (all values in GeV): $10-35$ (stands for 20), $55-65$ (60), $92-108$ (100), $140-160$ (150), $240-260$ (250), $450-550$ (500).

- Fig.15 shows the distributions of *Alpha* **parameter** for Monte Carlo gammas of different energies. Clearly, the FWHM of these distributions increases at lower energies as expected. We have a value of about $6°$ for energies of about 150 GeV (proposal: $5°$), while at 60 GeV it becomes $10°$, as for proposal, and ca. $16°$ at 20 GeV (proposal: $15°$).

- In the following figures 16 and 17, we can see that *Length* and *Width* increase gradually with energy. With respects to the proposal, we see that at *20, 100 and 500 GeV* the mean *Length* is $0.12°, 0.22°, 0.29°$ (proposal $(0.10-0.15)°, 0.22°, 0.27°$) and the mean *Width* $0.05°, 0.09°, 0.13°$ (proposal $0.06°, 0.08°, 0.12°$).

- Finally, in figure 18, the distribution of *Conc* is shown, that is to say the sum of the signal in the two highest pixels divided by *Size*. In the proposal a similar quantity was used, but counting the signal in the seven highest pixels. looking at the plots for gammas and protons it seems that both parameters may have about the same separation power.

- In the following figures 19,20,21, there is the behaviour of parameters *Length*, *Width* and *Conc*, in case of protons. Also here, in first approximation, there is no discrepancy with the proposal results.

These comparisons show reasonable agreement between the proposal predictions and the results of this simulation. This makes the difference in the estimate of the γ/h separation capabilities even more puzzling. Unfortunately there is not much documentation on what separation cut values were used in the former study, or how they were optimized.

6.1 Comparison of image parameter distributions for gammas and protons

Obviously, the distributions of image parameters at fixed energy bins for protons and gammas should not be directly compared in order to estimate their usefulness for hadron discrimination. In real data protons and gammas of all energies will be mixed together. We should either compare global distributions, or make cuts which can be done as well in the real data (as the *Size* cuts we have used in our study). Figures 22 to 26 present such a comparison. The distributions are made with the MC population remaining after the increasing size-cuts.

6.2 Is it possible to find better cuts with the same set of image parameters?

As a check of whether the gamma/hadron separation cut decided by the Random Forest method is working, we have plotted four of the most discriminating image parameters for gammas and hadrons after the gamma/hadron separation has been applied. This can be seen in figure 27. The distributions after the cut, if not identical, are similar enough as to show that there is little room for improving the separation by applying smarter cuts on the chosen set of image parameters. So, in our opinion, any future enhancement of the analysis will have to come from new parameters.

7 Importance of muons

Finally, we will briefly address the contribution of muons to the background of MAGIC. In the last version of the MC chain, new variables have been introduced in the final output which allow us to know what percentage of the light of any given event has been produced by muons. By histogramming this variable in the hadron events belonging to our basic sample (no *Size* cut), as in fig. 28, we see that at trigger level about 45% of events have no muon content at all ("muon-free" events). Then the histogram is more or less flat up to $\simeq 0.9$, and then rises again (21% of events have more than 90% of light produced by muons). We have checked that after gamma / hadron separation the percentage of muon-free events goes up to 73%. This means that supressing these remaining 27% of "muon" events, even if this is achieved with no loss of gamma events, will push down our sensitivity just by a factor 1.17 ($= 1/\sqrt{0.73}$).

The conclusion is that muons will not be such a big concern for MAGIC. This statement depends of course on whether all (or a large majority of) hadrons which can produce muons which can trigger MAGIC are actually contained in our MC sample. If more distant, or less energetic hadrons, can produce muons above the Cherenkov threshold pointing towards the telescope, the conclusion would not hold.

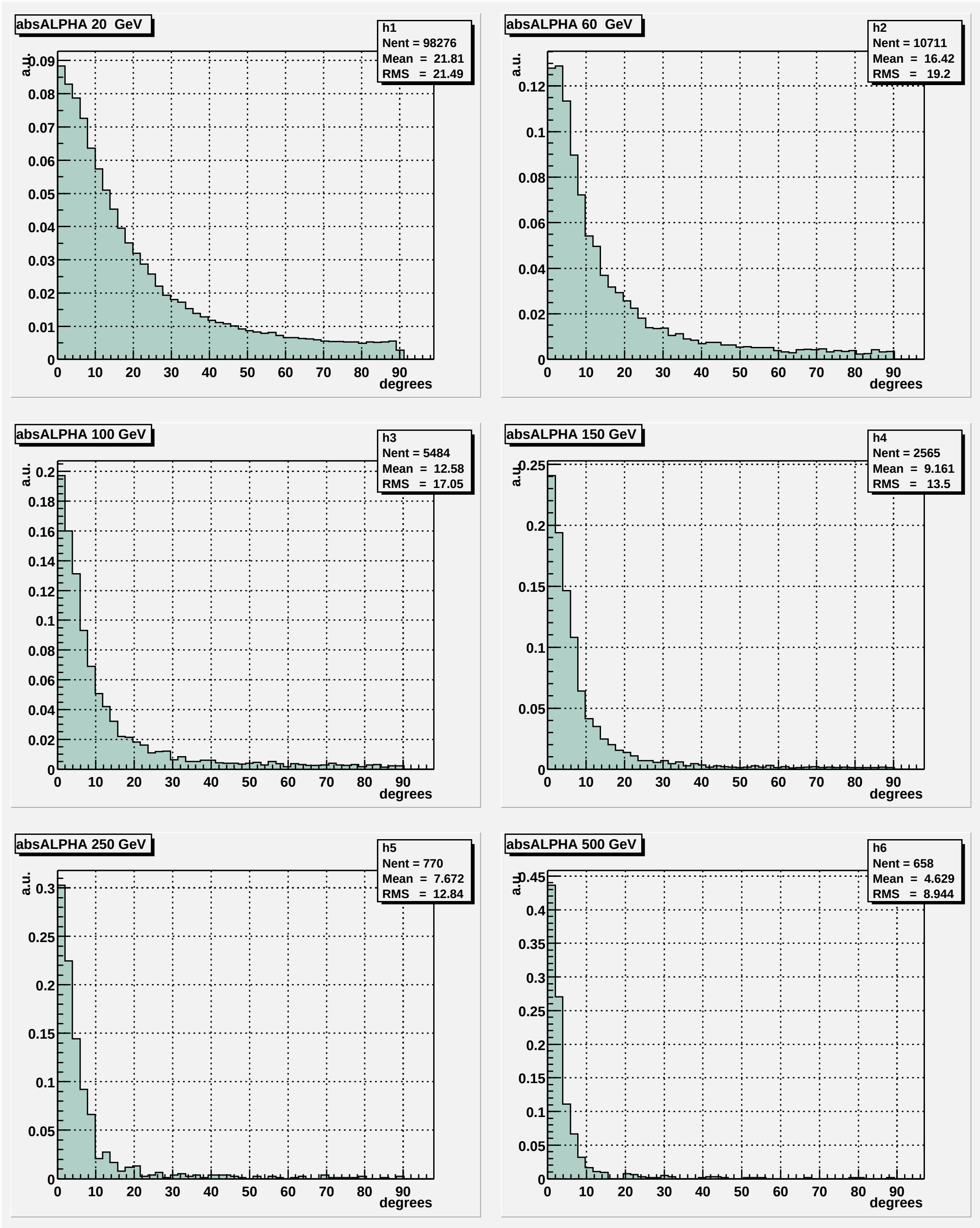

Figure 15: *Alpha* distributions for gammas of different energies.

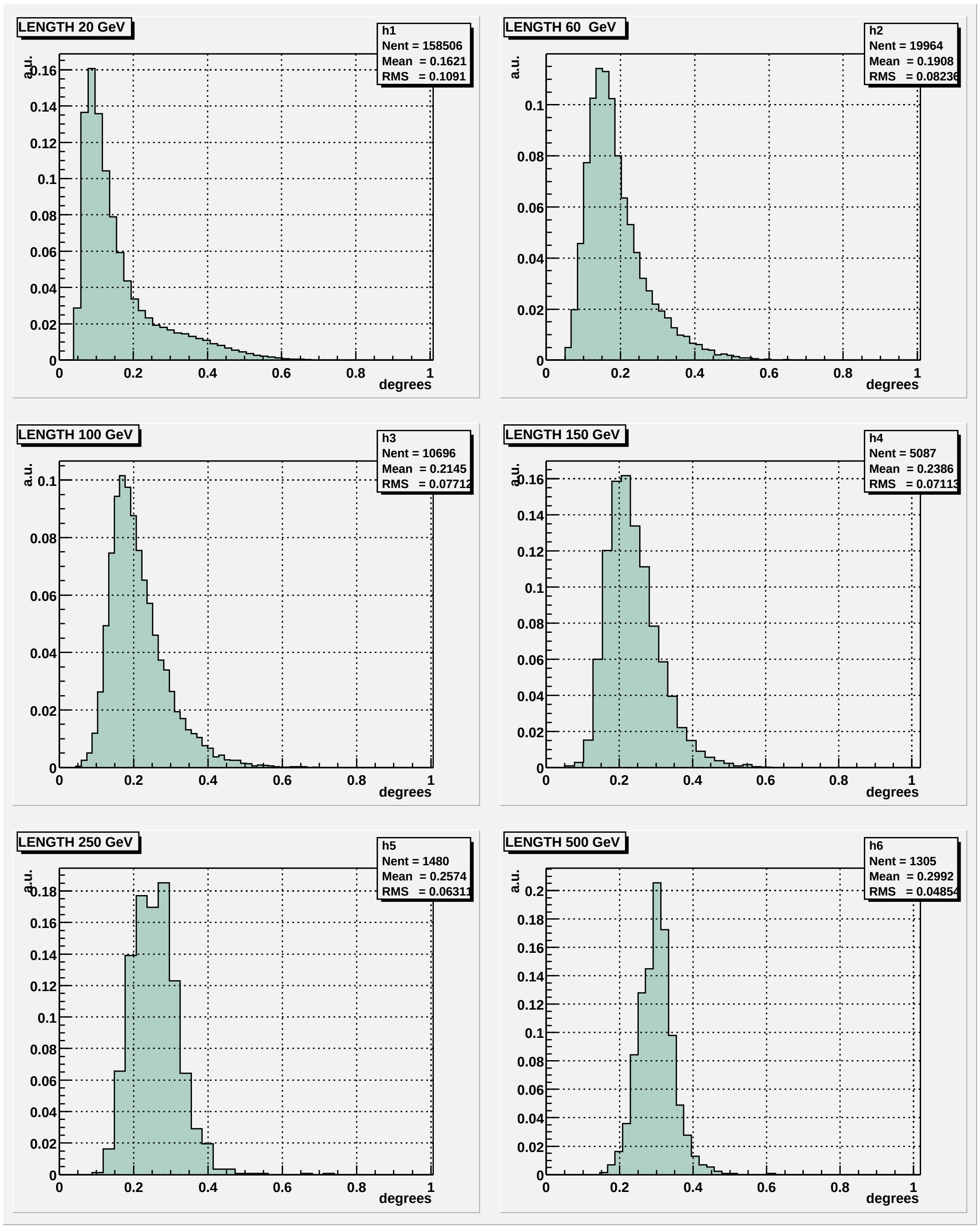

Figure 16: *Length* distributions for gammas of different energies.

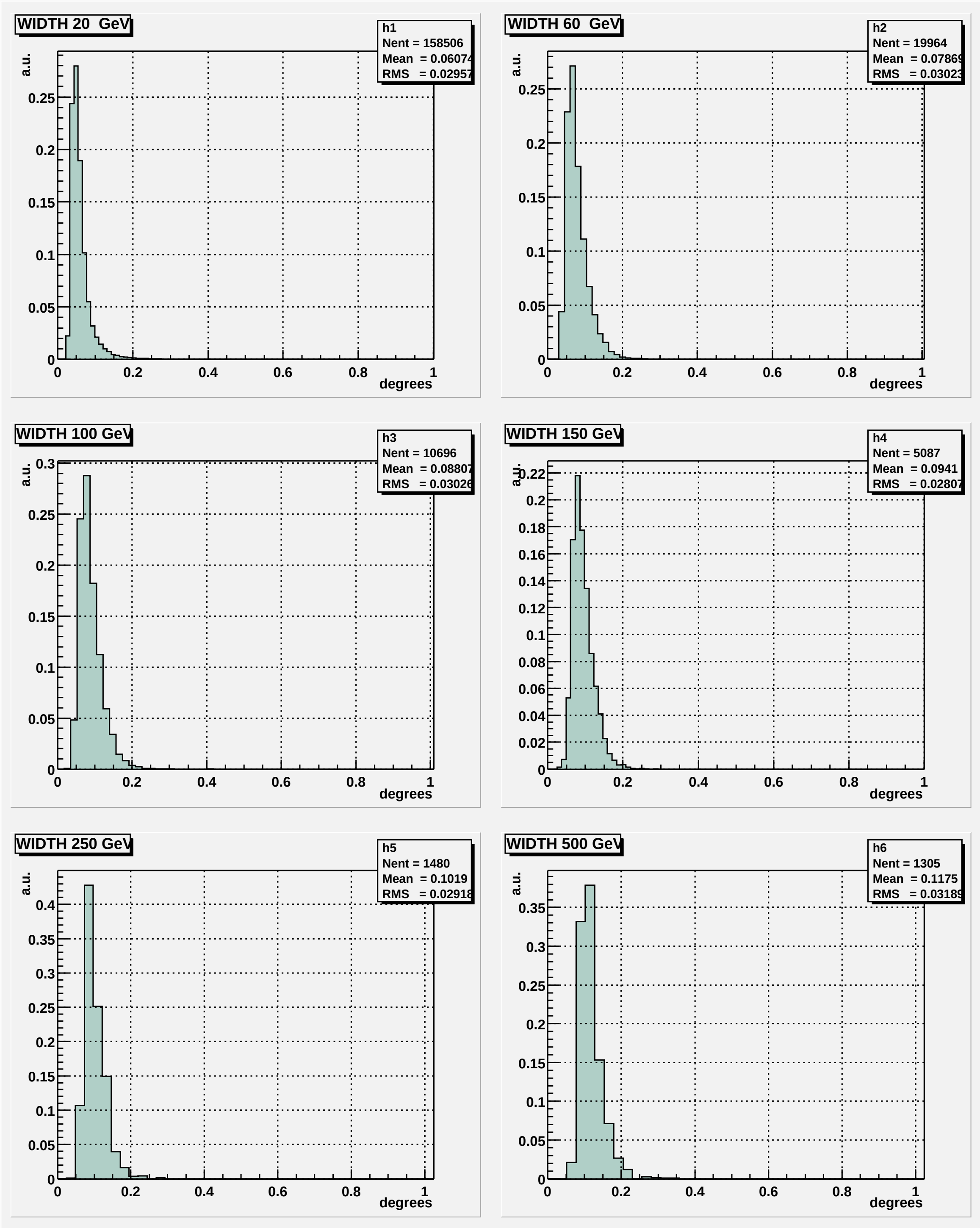

Figure 17: *Width* distributions for gammas of different energies.

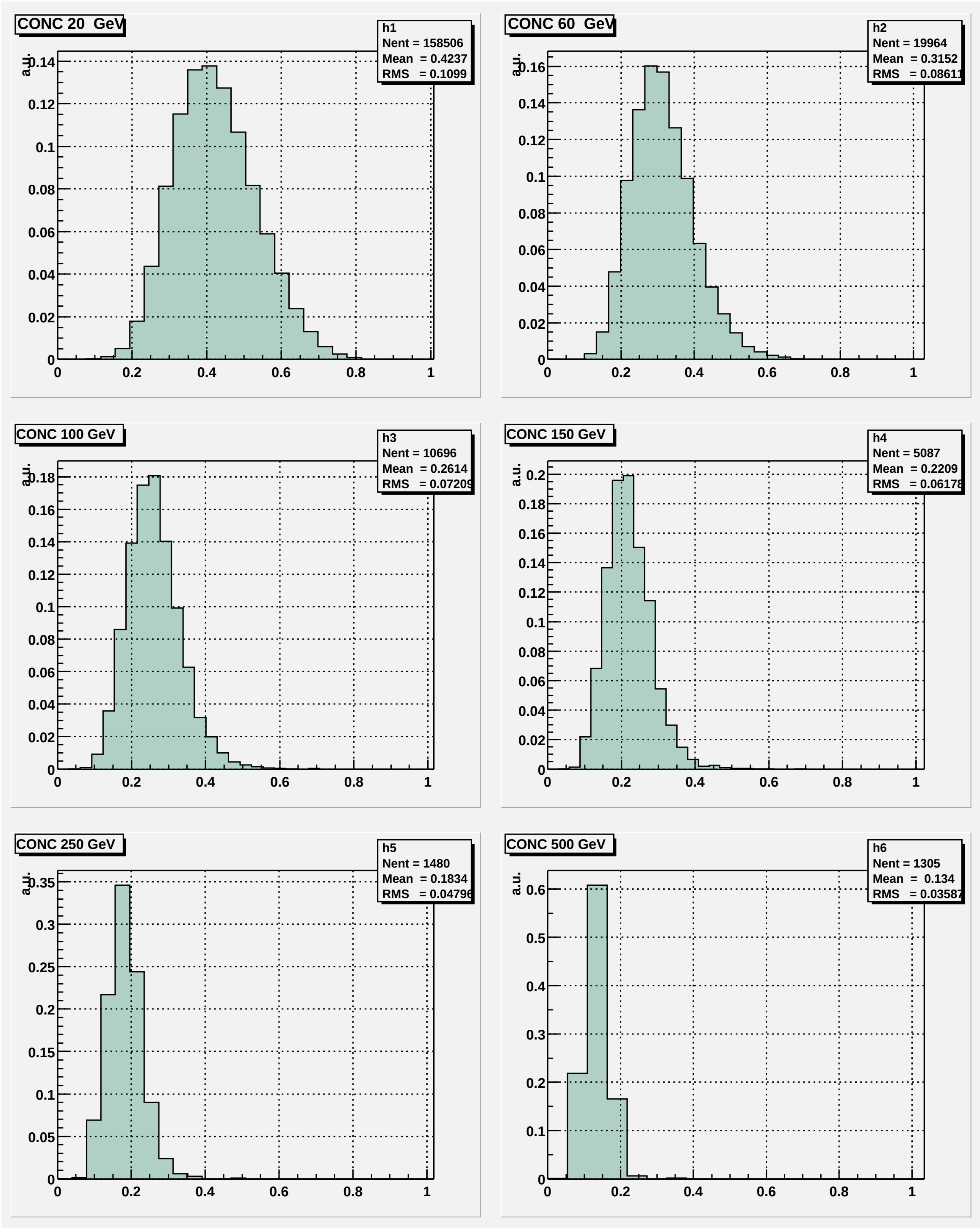

Figure 18: *Conc* distributions for gammas of different energies.

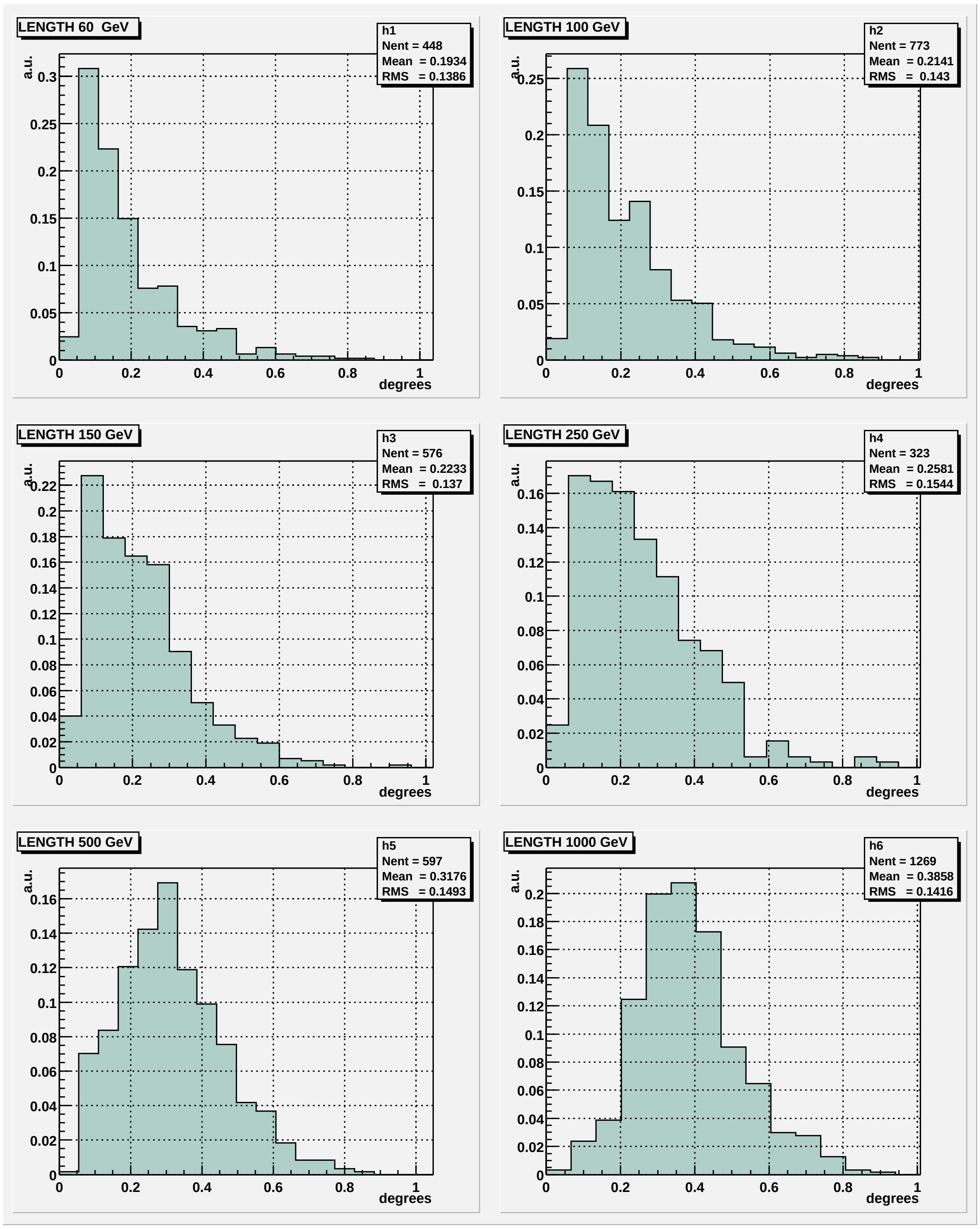

Figure 19: *Length* distributions for protons of different energies.

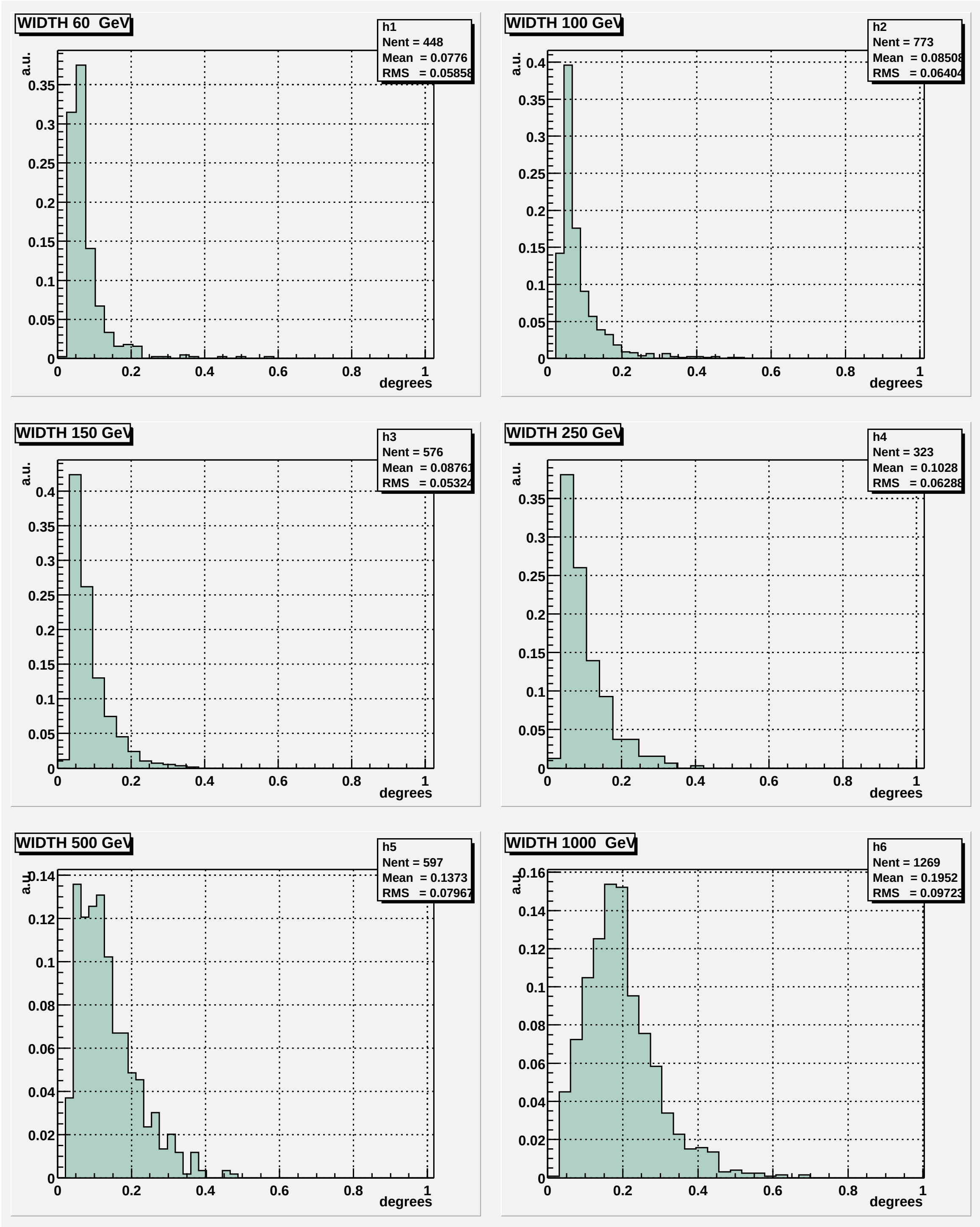

Figure 20: *Width* distributions for protons of different energies.

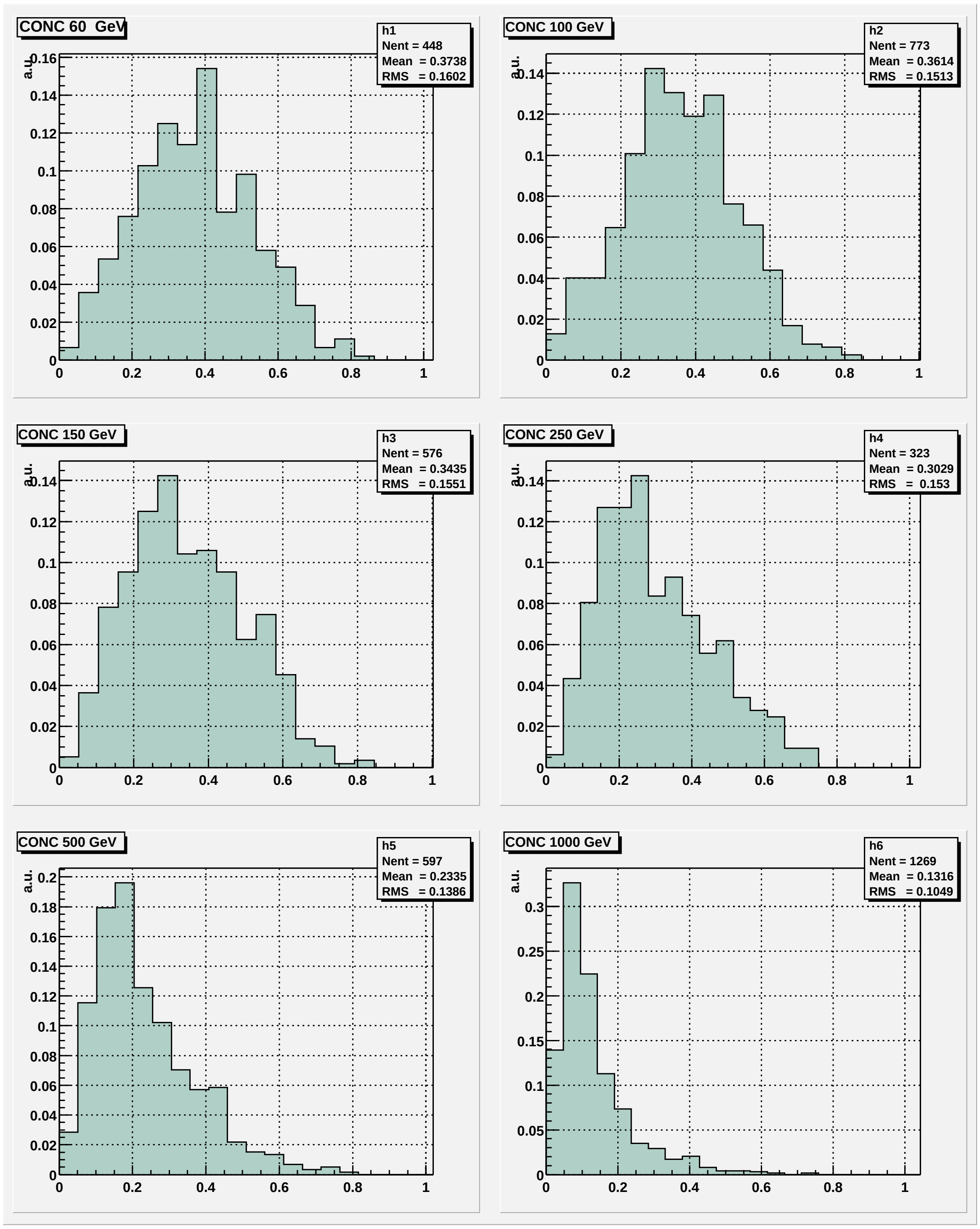

Figure 21: *Conc* distributions for protons of different energies.

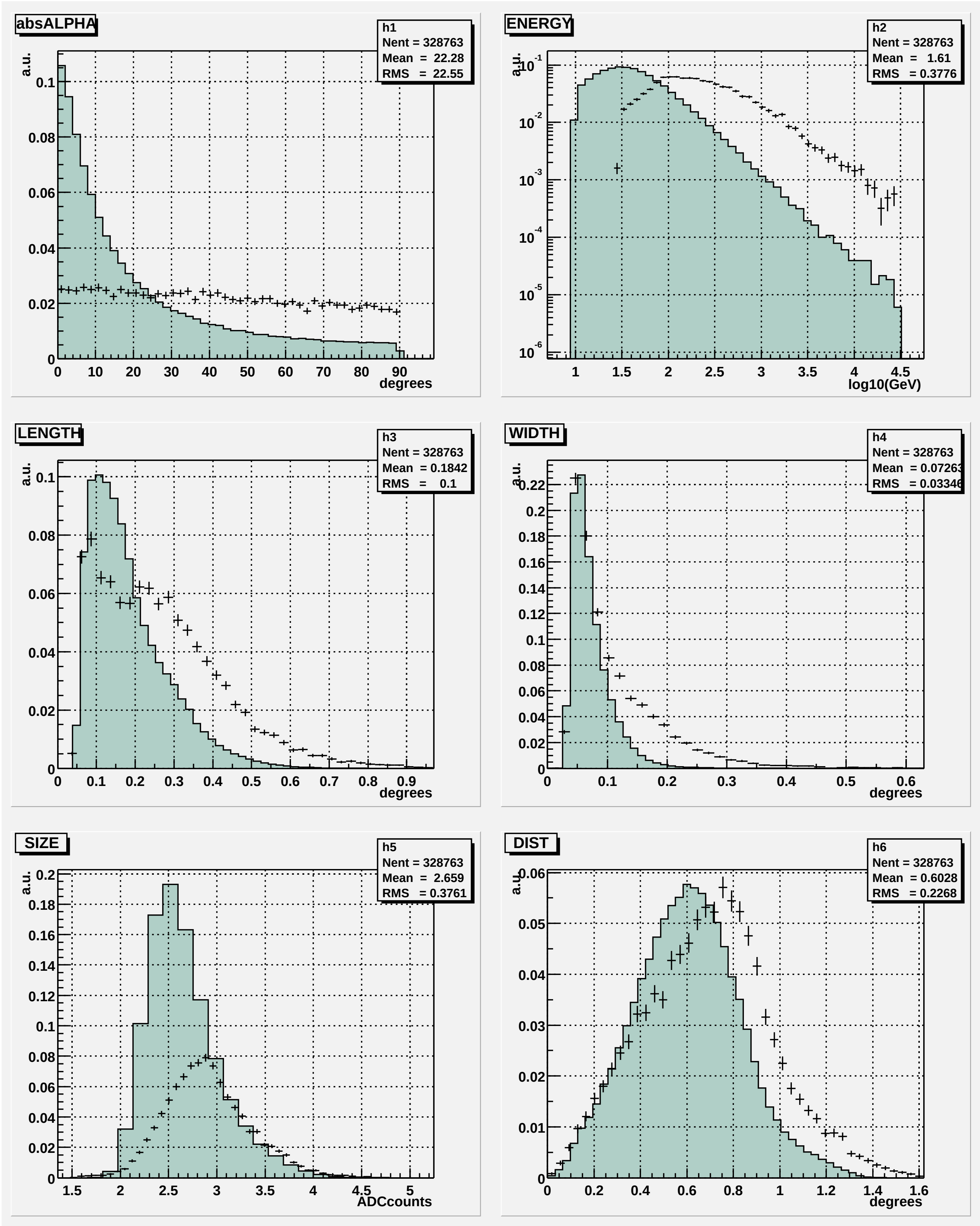

Figure 22: Global gammas and protons distributions of some Image parameters.

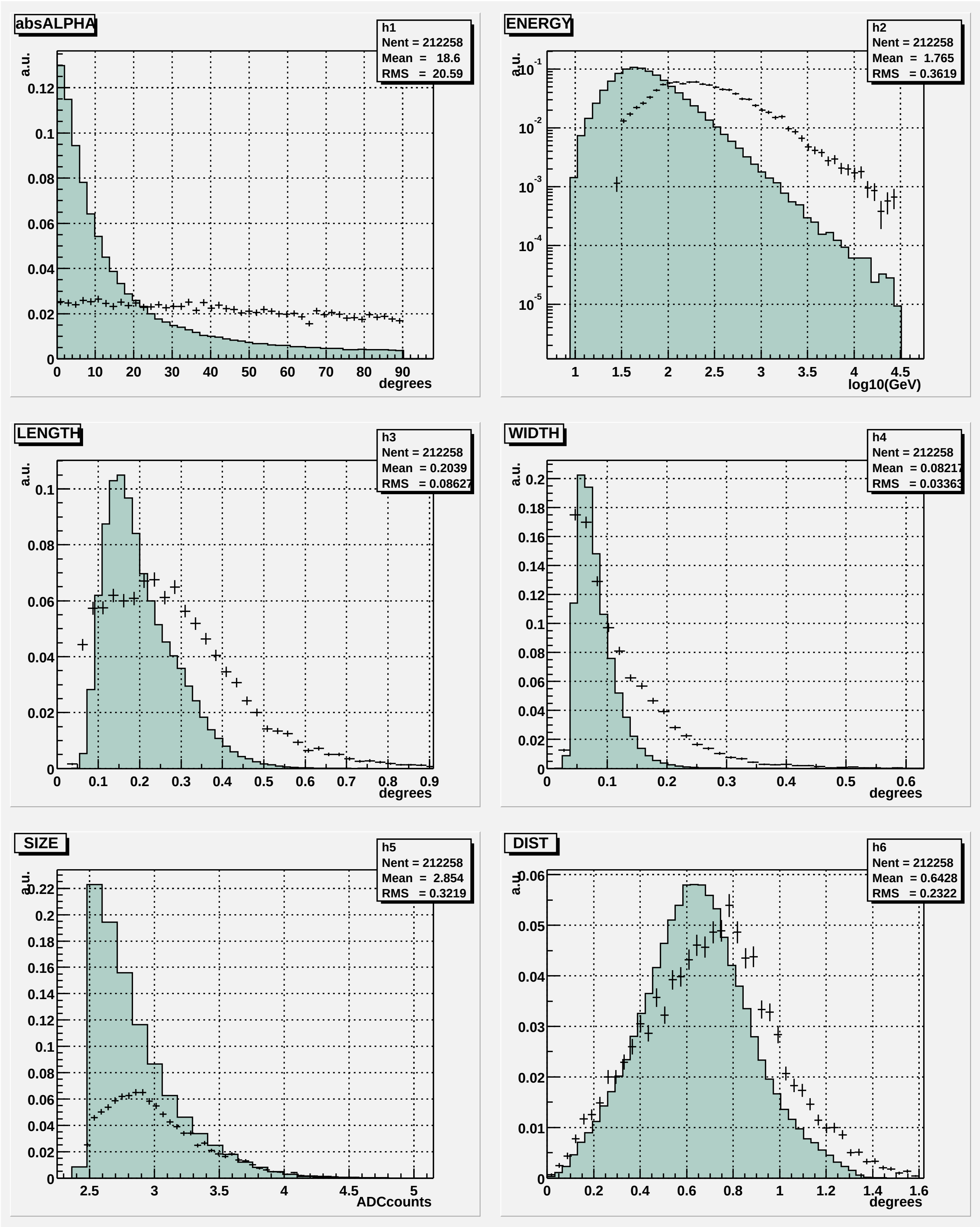

Figure 23: Gammas and protons distributions of some Image parameters for $Size > 300$ ADC counts.

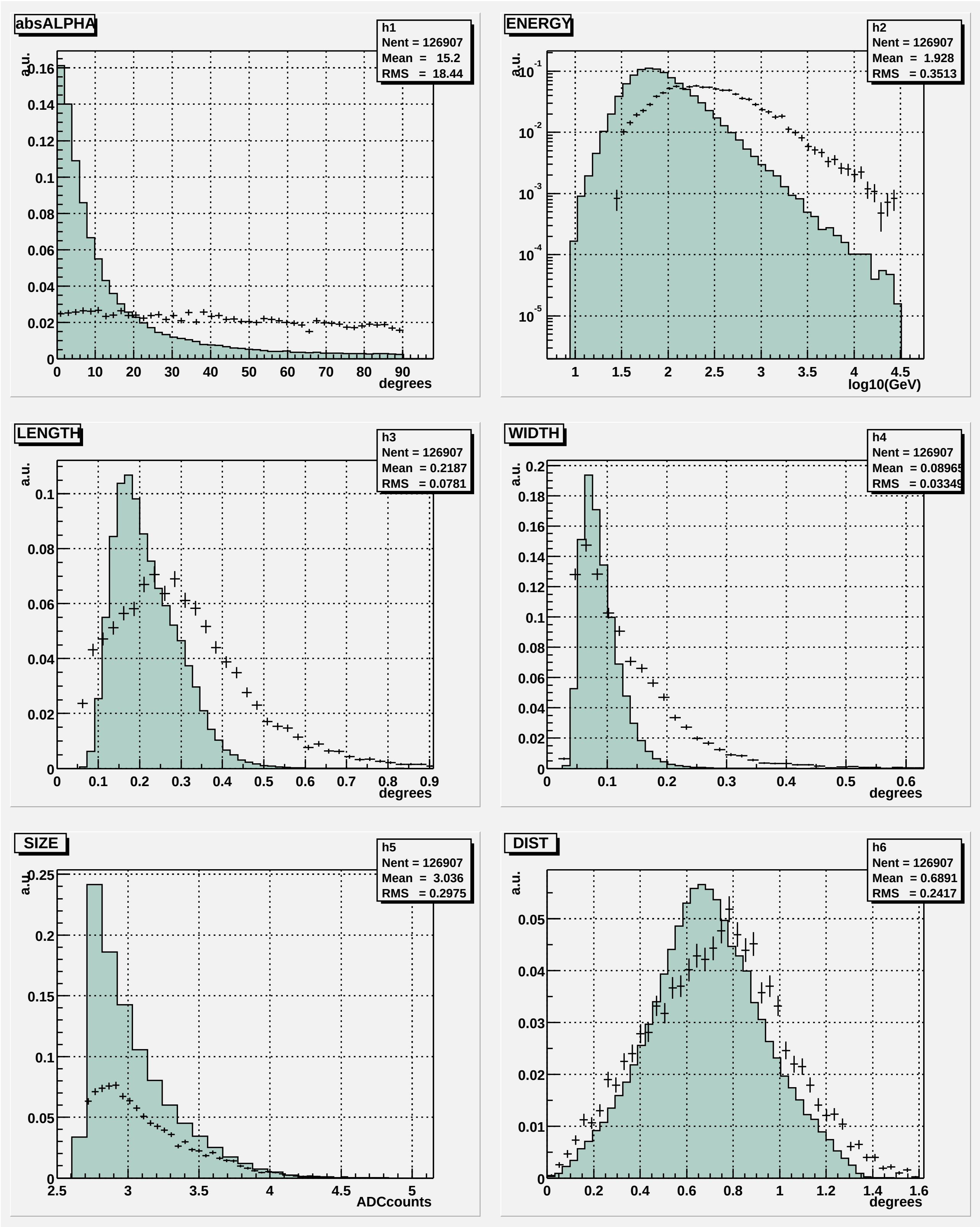

Figure 24: Gammas and protons distributions of some Image parameters for *Size* > 500 ADC counts.

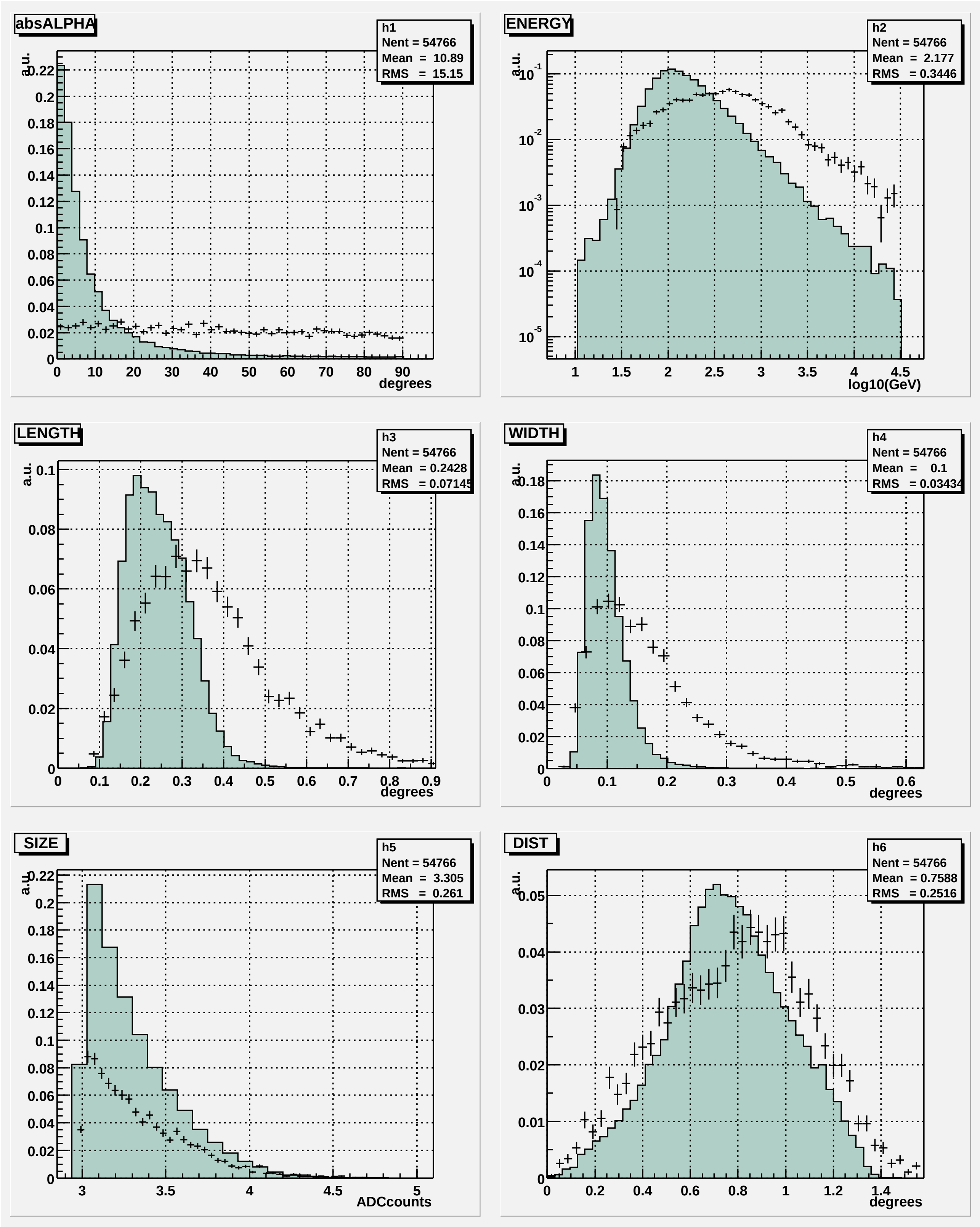

Figure 25: Gammas and protons distributions of some Image parameters for $Size > 1000$ ADC counts.

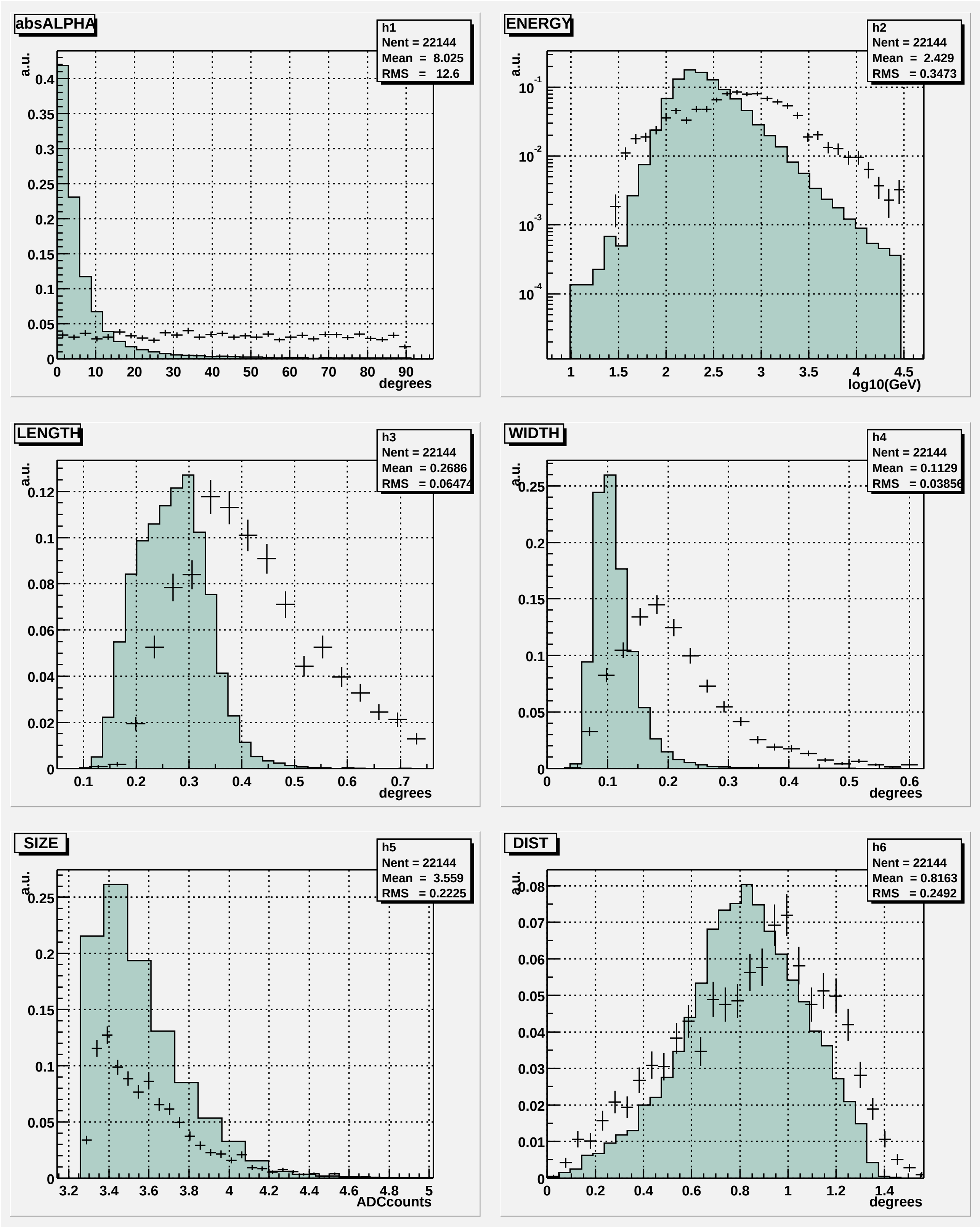

Figure 26: Gammas and protons distributions of some Image parameters for $Size > 2000$ ADC counts.

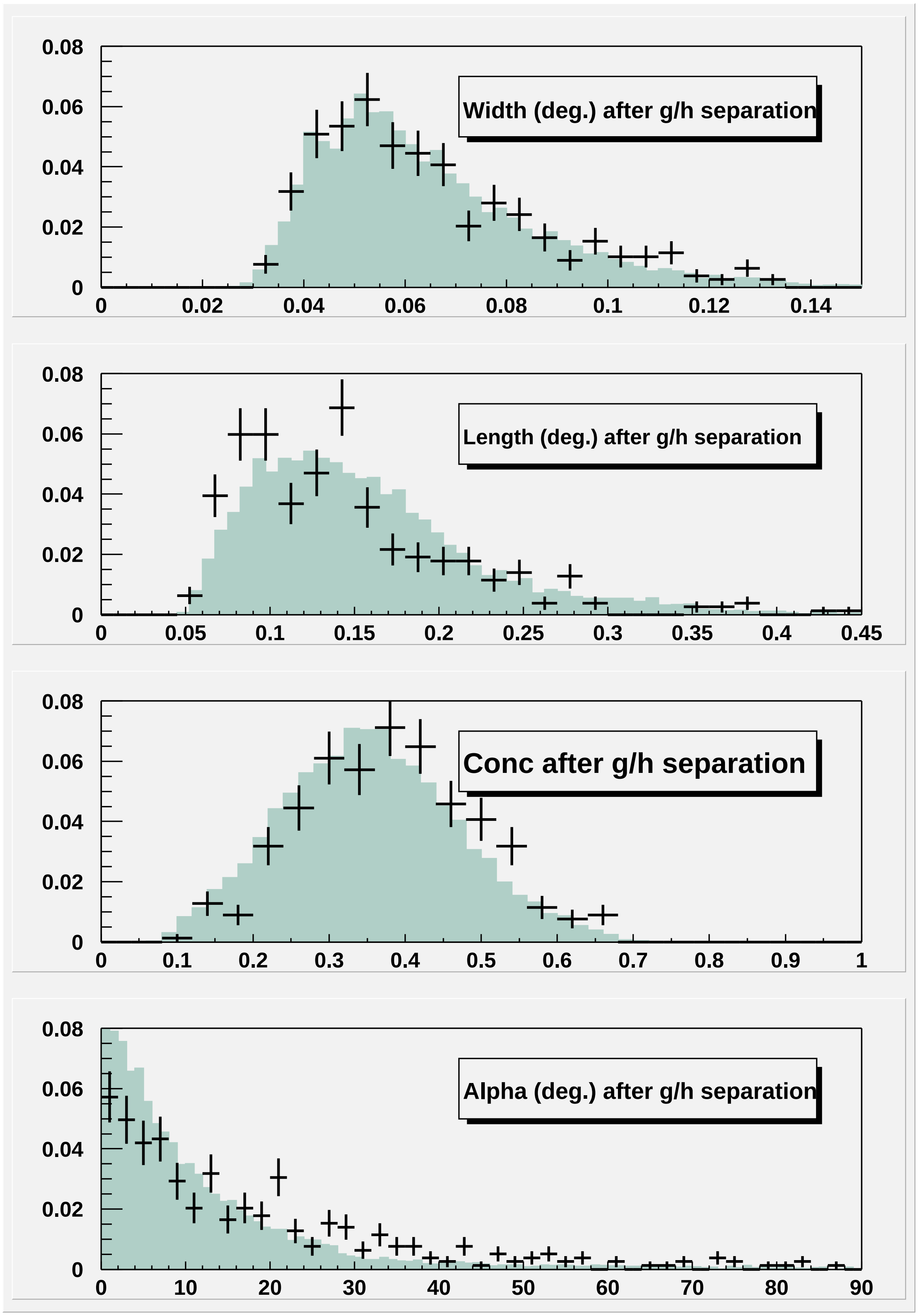

Figure 27: Distribution of some image parameters for gammas (green filled histograms) and hadrons (crosses), both after gamma/hadron separation (sample without *Size* cut).

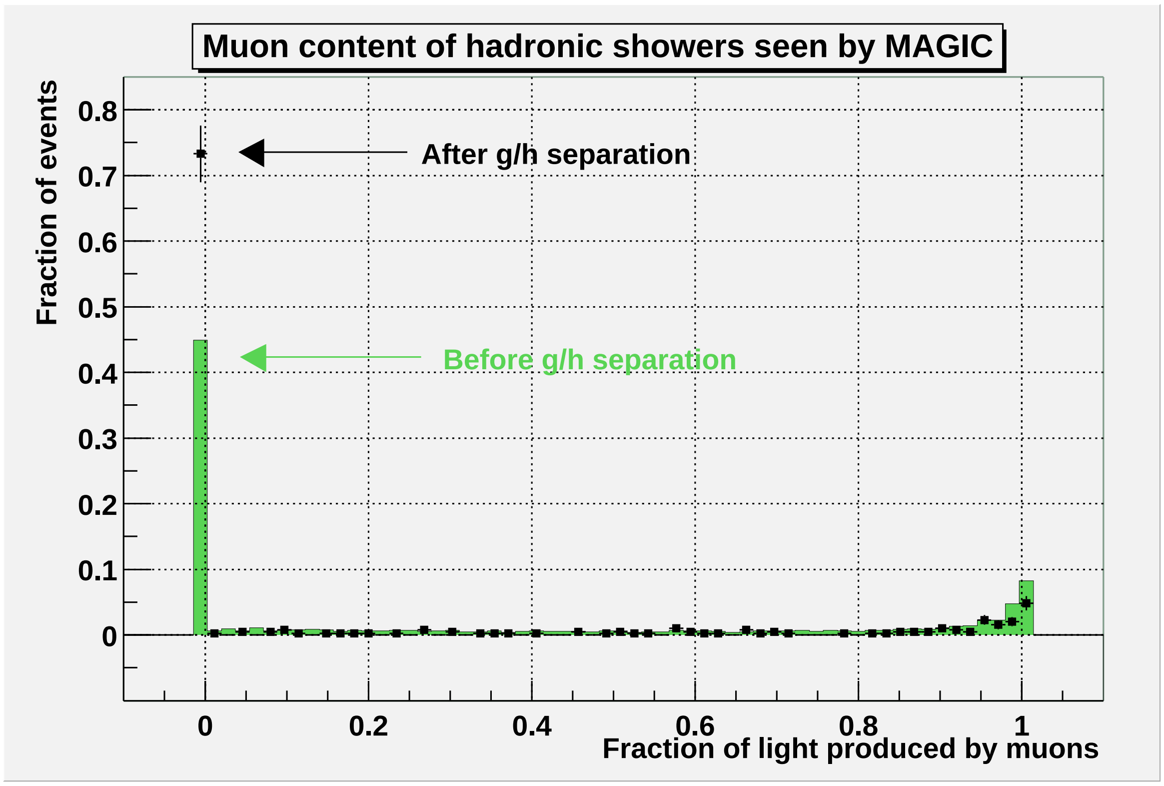

Figure 28: Histograms of the relative contribution of muons to the total light in hadronic showers, before and after gamma / hadron separation (sample without *Size* cut). It can be seen that after gamma / hadron separation more than 70% of the remaining showers have no muon content at all.